6-21-2023 11:00 AM

Investigating the Role of Endothelial BReast CAncer Susceptibility Gene 2 in Doxorubicin-induced Cardiotoxicity

Berk U. Rasheed, *Western University*

Supervisor: Singh, Krishna K., *The University of Western Ontario*

A thesis submitted in partial fulfillment of the requirements for the Master of Science degree in Anatomy and Cell Biology

ABSTRACT

Doxorubicin (Dox) is a chemotherapeutic drug used to treat various malignancies including breast and ovarian cancers. Accumulating evidence implicates cardiac impairments associated with Dox treatment. The *Breast Cancer Susceptibility Gene 2* (*BRCA2*) functions to maintain genome-wide stability by promoting DNA-damage repair. Accordingly, cardiomyocyte damage is specifically regulated by contributors of DNA damage repair such as *BRCA2*. The endothelium, the innermost cells of every blood vessel, act to protect our tissues from noxious elements, however, recent evidence suggests that *BRCA2* knockdown compromises endothelial cell function. A putative role of endothelial *BRCA2* during Dox-induced cardiotoxicity (DIC) remains unknown. We hypothesized that endothelial-specific loss of *BRCA2* will induce endothelial dysfunction and exacerbate DIC. Our findings indicate that Dox treatment promoted weight loss and induced cardiomyocyte dysfunction in endothelial-specific *BRCA2* knockdown mice *in vivo*, alongside profound endothelial dysfunction *in vitro*, and suggests a novel mechanism for DIC in the absence of *BRCA2*.

KEYWORDS

Endothelium, Doxorubicin, Cardiac dysfunction, Cardiotoxicity, BRCA2, Endothelial dysfunction

SUMMARY FOR LAY AUDIENCE

Changes in the genetic makeup of cells can increase one's susceptibility to the development of cancer. Mutations in the *BRCA2* gene, an important gene that maintains the integrity of the genome, have been implicated in the development of breast and ovarian cancers. *BRCA2* plays an important role in repairing DNA damage, and thus, when BRCA2 does not function as intended due to a deleterious change in the gene, there is an accumulation of DNA damage that increases the likelihood of breast or ovarian cancer development. The most used chemotherapeutic drug for breast cancer is Dox, an agent that kills tumour cells by causing DNA damage. Unfortunately, Dox has many undesirable side effects, the most severe of which is heart failure which raises concern about Dox use as a clinical therapeutic. The endothelium, or the innermost cell layer of our blood vessels, acts as a barrier to harmful agents from entering important tissues, like the heart. In people with *BRCA2* mutations, the endothelial barrier is compromised due to the accumulation of DNA damage in endothelial cells, and thus agents like Dox can access the heart at much higher concentrations. This results in cardiac cell death that can lead to heart failure, a fatal clinical outcome. This thesis aims to elucidate the role of BRCA2 in the endothelium and its importance in preventing endothelial dysfunction and cardiac dysfunction during Dox treatment. We employ a mouse model with *BRCA2* expression knocked down in endothelial cells and administer Dox to observe changes in mortality, cardiac functionality, and cardiac structure. Next, we employ endothelial cell culture systems to examine the functional mechanisms by which BRCA2 protects the endothelium in the presence of Dox. We found increased mortality and cardiac dysfunction in our BCRA2 knockdown mice exposed to Dox and Dox decreased the survival, proliferation, and tube formation in cultured endothelial cells. This thesis's findings provide important context for recognizing a critical role for BRCA2 in the endothelium in the protection of heart tissue.

ACKNOWLEDGEMENTS

I would like to thank my supervisor, Dr. Krishna Singh for his guidance, expertise, and support throughout my thesis. His encouragement during tough times helped me persevere and overcome the many challenges that arose from my thesis. I would also express special thanks to David Michels and Dr. Lynn Wang for their kindness and help with the establishment of the project before I took the reigns. I would like to also thank my lab peers, Hien Nguyen, and Sepideh Nikfarjam, for their emotional and technical support during troubling times. My advisory committee members, Dr. Alison Alan and Dr. David Hess were amazing pillars guiding my scientific mind. I wholly appreciate their expertise and viewpoints during our committee meetings. A special thanks to Dr. Martin Duennwald for his role as my GAC representative and lab neighbour. This work was made possible with funding from the Canadian Institute of Health Research (CIHR) and the Western Graduate Research Scholarship (WGRS).

TABLE OF CONTENTS

LIST OF ABBREVIATIONS

aMHC	Alpha myosin heavy chain
ANOVA	Analysis of variance
ATM	Ataxia-telangiectasia mutated
ATR	ataxia-telangiectasia Rad3
bMHC	Beta myosin heavy chain
BNP	Brain natriuretic protein
BRCA	Breast cancer susceptibility gene
BRCA2	Breast cancer susceptibility gene 2
cDNA	Complementary DNA
Ckmt2	Creatine kinase S-type, mitochondrial
CtIP	BRCA1–CtBP-interacting protein
DIC	Dox-induced cardiotoxicity
Dox	Doxorubicin
DSB	Double-stranded breaks
EC	Endothelial cells
eNOS	Endothelial nitric oxide synthase
FABP3	Fatty acid binding protein-3
Glul	Glutamate-ammonia ligase
H&E	Hematoxylin & Eosin
H2AX	Histone family member X
HCAECs	Human coronary arterial endothelial cells
HRR	Homologous recombination repair
HUVECs	Human umbilical vein endothelial cells
ICAM-1	Intracellular adhesion molecule 1
IFT88	Intraflagellar transport protein 88
IP	Intraperitoneally
LFA-1	Lymphocyte function-associated antigen 1
LV	Left ventricular
LVEDD	Left ventricular end dyastolic dimension
LVEF	Left ventricular ejection fraction
LVESC	Left ventricular end systolic dimension
LVFS	Left ventricular fractional shortening
MRN	MRE11–RAD50–NBS1
Myl2	Myosin light chain 2
NBS1	Nijmegen breakage syndrome protein 1
NRF2	Nuclear factor erythroid 2-related factor 2
oxLDL	Oxidized LDL
p53	Tumour protein 53
PALB2	BRCA1–partner and localizer of BRCA2

1 BACKGROUND

1.1 BRCA1/2 and Cancer

The *Breast Cancer Susceptibility Genes* (**BRCA**) 1 and 2 are classified as tumour suppressors and are crucial members of the genome surveillance complex (Alacacioglu et al., 2018). Mutations in the *BRCA* genes significantly increase the risk of familial and/or early-onset cancer (Baretta et al., 2016; Hughes et al., 2005). *BRCA* mutations account for 50-85% lifetime risk of breast cancer and 15-40% lifetime risk of ovarian cancer development (Gast et al., 2018). *BRCA1* mutations also confer an increased risk of gastric cancers, whereas *BRCA2* mutations are associated with a greater risk of pancreatic and prostate cancers compared to the general population (Foulkes, 2008; Kuchenbaecker et al., 2017).

1.2 BRCA1/2 and Homologous Recombination Repair

The *BRCA1* and *2* gene products are structurally distinct and function independently of one another. The *BRCA1* gene is located on the long arm of chromosome 17 at position 21.31 (17q21.31) encompassing 22 exons coding for a 220 kDa protein. The *BRCA2* gene is located on the long arm of chromosome 13 at position 12.3(13q12.3) and contains 26 exons that produce a 384 kDa protein (Yoshida & Miki, 2004). The BRCAs primary roles are to maintain cellular and genomic stability (Boulton, 2006). When BRCA1/2 functionality is compromised, tumorigenesis is promoted (Venkitaraman, 2019). The *BRCA* genes modulate critical roles in homologous recombination repair (**HRR**), a mechanism aimed at the repair of double-stranded breaks (**DSB**s) (Zhao et al., 2019). Furthermore, HRR is the only known pathway whereby BRCA1 and 2 are known to interact thus far.

The HRR pathway begins with a DSB in DNA. A sensing complex, known as the histone family

member X (**H2AX**), associates near the site of DNA damage, and the progression of HRR is dependent on the association of a complex comprised of BRCA1 with phosphorylated H2AX, which is the mediator of the DNA damage checkpoint protein and RING finger protein 8. Following the sensor complex initiation, a mediating complex that resects DSBs from 5' to 3' begins with the formation of the BRCA1–CtBP-interacting protein (**CtIP**) complex associating with the **MRN** complex [comprised of MRE11–RAD50–**NBS1** (Nijmegen breakage syndrome protein 1)]. The product is the formation of a 3' single-stranded DNA that associates with replication protein A (**RPA**) to prevent it from binding to other single-stranded DNA molecules. The effectuating complex is RAD51-dependent and is recruited via the BRCA1–partner and localizer of BRCA2 (**PALB2**)–BRCA2 complex, where in most somatic cells is non-crossover synthesis-dependent strand annealing (Nikfarjam & Singh, 2023). The role of the BRCAs, especially that of BRCA1, does extend past HRR. For instance, tumour protein 53 (**p53**)-dependent cell cycle checkpoints are activated in response to DNA damage that is recognized by ataxia-telangiectasia mutated (**ATM**) and Rad3 (**ATR**) kinases, which phosphorylate BRCA1 and begin complex formation that initiates said checkpoint activation in the S and G2/M phases (Roy et al., 2012). The role of BRCA2 in cell cycle checkpoint activation is suggested to be indirect, whereby genetic instability caused by dysfunctional BRCA2 can result in additional deleterious mutations in checkpoint proteins, including those in p53 (Marmorstein et al., 2001).

When HRR is compromised, there is a systemic accumulation of DNA damage that can promote cell cycle arrest, cellular senescence, tumorigenesis, or apoptosis (Kawale & Sung, 2020; Takaoka & Miki, 2018; Zhao et al., 2019). Both BRCAs have been implicated in important processes such as inflammation and apoptosis demonstrated by studies showing increased BRCA mRNA and protein levels in these processes (Shukla et al., 2011; K. K. Singh et al., 2012). Furthermore, the

clinical outcomes of patients with deficient/dysfunctional BRCAs are much worse than those without (Baretta et al., 2016; Y. Zhu et al., 2016). Patients with deficient/dysfunctional BRCAs also have higher incidences of cardiovascular diseases, diabetes, hypertension, hypercholesteremia, etc. (Bordeleau et al., 2011; Liao et al., 2013; W. Wang et al., 2021).

1.3 BRCA1/2, Anthracyclines, and Cardiotoxicity

The choice of therapy for breast and ovarian cancer patients is dependent on multiple factors including, but not limited to **BRCA1/2** mutation status, age, diabetic status, and the use of other medications (Cain et al., 2017; Nagini, 2017; Sarhangi et al., 2022; Sener, 1996). Anthracyclines are the most used chemotherapeutics for the treatment of breast and ovarian cancers (Shah & Gradishar, 2018). Anthracyclines are a class of chemotherapeutic drugs that function via inhibition of topoisomerase II and by intercalating between replicating DNA strands. Doxorubicin (**Dox**) is the most frequently utilized anthracycline for the treatment of breast cancer; however, its usage is carefully considered due to several patients experiencing cardiotoxicity, a condition referred to as Dox-induced cardiotoxicity (**DIC**). Approximately 5% of Dox recipients experience heart failure, a fatal outcome with little or no treatment options available (Kim et al., 2018; Rawat et al., 2021; Shah & Gradishar, 2018). The mechanisms of DIC have not been clearly understood so far, however, some of the suggested mechanisms include cardiomyocyte apoptosis secondary to Dox-induced DNA damage, generation of double-stranded breaks via Dox-induced DNA interstrand cross-linking, enhanced production of reactive oxygen species (**ROS**) [e.g., via Dox-Fe complex formation, mitochondrial-dependent and NAPDH dependent ROS formation], intracellular calcium dysregulation, dysregulation of autophagy, and activation of the tumor suppressor p53 in cardiomyocytes (Rawat et al., 2021).

There are limited yet contradictory and alarming reports regarding the usage of anthracyclines in

BRCA1/2 mutation carriers and cardiovascular complications. For instance, Demissei *et al*. and Pearson *et al*. report no changes in cardiovascular function or fitness in breast cancer survivors administered Dox with *BRCA1/2* mutations versus the general population (Demissei et al., 2022; Pearson et al., 2017). In contrast, Ahmad *et al.*, MacDonald *et al.*, and Ruddy *et al.*, all report significantly higher incidences of heart failure in *BRCA1/2* mutation carriers (Ahmad et al., 2012; MacDonald et al., 2013; Ruddy et al., 2017). There are varying reasons why contradictory findings are being reported, such as the age of anthracycline administration, the presence of cardiovascular disease comorbidities, and diabetes status. However, another mechanistic insight into this phenomenon may be genetic haploinsufficiency. Genetic haploinsufficiency may be a product of not only a non-functional allele but also the failure of a functional allele to sufficiently compensate for reduced *BRCA* expression (Johnson et al., 2019). These patients may not always be detected in screening tests for *BRCA1/2* mutation statuses and may subsequently be characterized as healthy control patients, thus skewing the reports to statistical insignificance between the general population and *BRCA1/2* mutation carriers.

The increased risk of cardiovascular complications is not only limited to the administration of anthracyclines but also to chest radiotherapy and HER2-directed therapies (e.g., trastuzumab has also been associated with induced heart failure (Nicolazzi et al., 2018)) (Jerusalem et al., 2019; Koutroumpakis et al., 2020). Accordingly, these therapeutics can also be administered to *BRCA* haploinsufficient patients depending on the mechanism of target for their cancers. The commonality of these therapies is their collective role in inducing DNA damage in highly replicative cells while being harmful to non-replicative cells such as cardiomyocytes in higher concentrations. Cardiomyocytes are the functional units of the heart, responsible for its contractility and subsequent systole and diastole. Cardiomyocytes do not proliferate following

injury/death; thus, cardiomyocyte death can lead to a multitude of pulmonary and cardiovascular complications (Woodcock & Matkovich, 2005).

The loss of *BRCA2* in cardiomyocytes and DIC has been investigated. Singh et al. reported that cardiomyocyte-specific loss of *BRCA2* in mice resulted in reduced contractility and cardiac output, which was further exacerbated upon Dox administration (K. K. Singh et al., 2012). These mice displayed increased expression of p53 and other apoptotic molecules (Lorenzo et al., 2002). So far, studies have been mainly focused on cardiomyocytes, but recently shifted to investigate the role of the endothelium in Dox-induced toxicity; upon intravenous injection, the endothelium, the innermost layer in the lumen of blood vessels, is exposed to the deleterious effects of Dox (A. Z. Luu et al., 2018).

1.4 The Endothelium

The endothelium is a subset of cells that form the innermost layer of all vasculatures. Endothelial cells (**EC**s) have different shapes, genetic expression profiling, and function depending on their developmental origin and structure based on their location in the blood vessel (Dyer & Patterson, 2010).

These distinct differences vary from the structural composition of the ECs to their function. For instance, arterial ECs are generally thicker than venous ECs, where they are longer and more ellipsoidal. Venous ECs tend to be short and wide (except in high endothelial venules, where ECs are plump and cuboidal) (Florey, 1966). The difference in shape is a testament to the variation in blood flow, whereby in arteries blood flow is quick and undisturbed and in veins is significantly slower (Busse & Fleming, n.d.).

ECs are also heterogeneous depending on their developmental location within the body. Jambusaria et al. utilized RNA sequencing in mouse brain, heart, and lung ECs and found differing

transcriptomic profiles (Jambusaria et al., 2020). They found increased molecular heat map signatures for glycolysis genes in brain ECs (consistent with the brain's heavy consumption of glucose) and increased heat signatures for fatty acid metabolism (consistent with the heart's reliance on fatty acids in ATP generation). Interestingly, ECs also seemed to be involved in the function of the organ of interest. In brain ECs, *glutamate-ammonia ligase* (***Glul***) was upregulated and highly enriched, indicating ECs are involved in synaptic organization. Glul is an important protein implicated in the transportation and synaptic organization of excitatory neurotransmitters such as glutamate. In the lungs, ECs upregulated *surfactant protein C* and *mucin 1*, indicating an important interactive role between the parenchymal epithelium and ECs. In the heart, ECs upregulated genes involved in cardiomyocyte contraction, *myosin light chain 2* (***Myl2***) and *creatine kinase S-type, mitochondrial* (***Ckmt2***), suggesting a role of the cardiac endothelium in modulating cardiac contractility. However, all three EC subtypes had similar expression profiling of leukocyte migration genes, chemotaxis genes (e.g., *intracellular adhesion molecule 1 (**ICAM-1***) and *vascular cell adhesion molecule 1* (***VCAM-1***)), and leukocyte integrins (e.g., *lymphocyte function-associated antigen 1* (***LFA-1***) and *very late antigen 4* (***VLA-4***)), suggesting a shared mechanistic program of inflammatory processes in response to systemic stressors. However, veins, specifically post-capillary venules, are the sites where permeation occurs during inflammation (Majno & Palade, 1961). Leukocyte infiltration seems to primarily occur in post-capillary venules rather than arterial vessels due to lower flow rate, thinner walls, and fewer tight junctions (Nicolaides, 2005).

Altogether, the differing roles, mechanisms of function, and genotype profiles suggest a heterogenous response to external and internal stressors, warranting that studies of endothelial cells employ models from both arterial and venous origin.

1.5 Endothelial dysfunction

Endothelial dysfunction and death (endotheliotoxicity) involve increased inflammation, oxidative stress, and apoptosis (Ballinger et al., 2002; Lord & Bobryshev, 2002; Marrocco et al., 2017). Endothelial inflammation is characterized by increased E-selectin, VCAM-1, and intercellular adhesion molecule 1 expression (L. Wang et al., 2022). These markers of endothelial inflammation are increased during the inflammatory process induced by different risk factors such as angiotensin II (hypertension), oxidized LDL (**oxLDL**, atherosclerosis), and high glucose (diabetes) (Khan et al., 1995; Taki et al., 1996). ROS and increased oxidative stress are also significant contributors to endothelial dysfunction. ROS act as important signaling molecules that are produced as reactive intermediates from oxygen; however, when natural antioxidant defense systems cannot restore imbalances of ROS that arise, endothelial dysfunction occurs (Incalza et al., 2018). Moreover, impaired ROS homeostasis is the primary cause of endothelial dysfunction, resulting in vascular damage in metabolic and atherosclerotic diseases (Zheng et al., 2022). Endothelial apoptosis can be triggered by a multitude of factors such as p53-mediated checkpoint activation, the activation and accumulation of cleaved-caspase 3, mitochondrial dysfunction, and inflammation (Knapp et al., 2019; Lin et al., 2020; Lorenzo et al., 2002; Salnikova et al., 2021).

1.6 The Role of endothelial BRCA2

As mentioned previously, loss of BRCA2 function results in the accumulation of DNA damage. Dysfunctional BRCA2 leads to failure of the repair complex to recruit the effector of HRR, RAD51, and thus appropriate repair does not occur. The accumulation of DNA damage can result in endothelial cell dysfunction, inflammation, senescence, and apoptosis. However, the cell's fate is dependent on additional factors, primarily cell cycle checkpoint activation in the G2/S phase that is mediated by a pro-apoptotic protein, p53. If the checkpoint is active or p53 is intact/non-mutant,

the cell's fate leads toward apoptosis upon HRR failure (Gottlieb & Oren, 1998; Nicolai et al., 2015). The loss of *BRCA2* is also associated with the inhibition of endothelial nitric oxide synthase (**eNOS**), leading to cellular dysfunction (S. Singh et al., 2020). Heijink et al. cite that the loss of BRCA2 results in increased production and activity of micronuclei (Heijink et al., 2019), which are small nuclear membrane-bound compartments with DNA contents near the primary nucleus. Micronuclei have long been associated with chromosome instability, genome rearrangements, and mutagenesis (Krupina et al., 2021). These micronuclei have also been associated with increased production of tumor necrosis factor-alpha **(TNFα**), which can lead to inflammation, apoptosis, and cellular dysfunction (Muhammad et al., 2021). Interestingly, loss of *BRCA2* has also been shown to inhibit the antioxidant pathway nuclear factor erythroid 2-related factor 2 (**NRF2**), a master transcription factor that results in the expression of antioxidant genes functioning together to maintain ROS homeostasis, leading to the accumulation of ROS (Ma et al., 2012). A previous study from our lab demonstrated a protective role for *BRCA2* in ECs exposed to oxidative stress induced by oxidized low-density lipoproteins (S. Singh et al., 2020). This fundamental study revealed an urgent need for further assessment of the role of endothelial *BRCA2* under external stressors such as Dox.

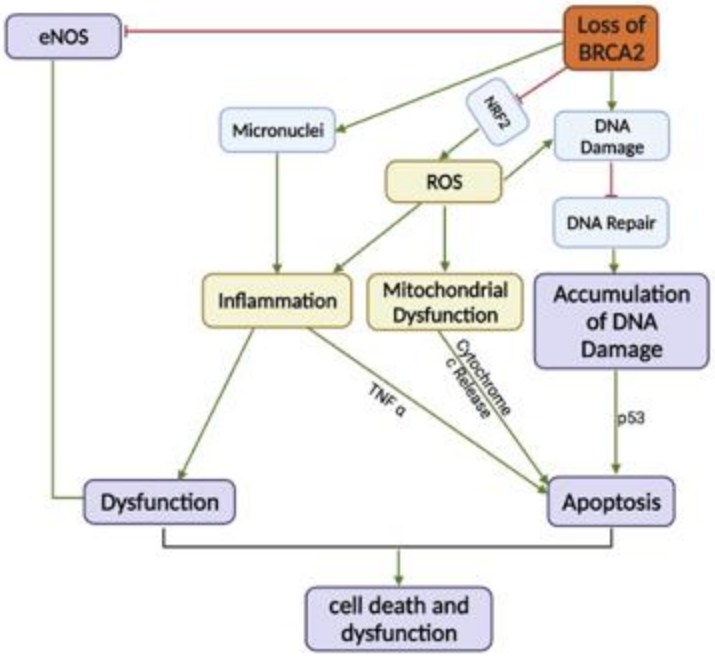

Figure 1. Schematic depicting the mechanistic role of the loss of *BRCA2* in cell death and dysfunction.

1.7 The Interactive Mechanisms of BRCA2 and Dox within the Endothelium

The endothelium is among the first tissue exposed to any intravenously introduced agents into the blood such as Dox, and thus compromised endothelial structure can lead to increased endothelium permeability, providing more access for noxious agents to infiltrate into other tissues such as the myocardium. Under normal conditions, the cardiac endothelium is relatively impermeable due to the presence of tight junctions, preventing harmful compound exposure to the myocardium (Wallez & Huber, 2008). However, circulating Dox can increase overall permeability by reducing the integrity of tight junctions (A. Z. Luu et al., 2018). This was demonstrated by Wilkenson et al. where the expression of the tight junction protein zona occludens 1 (**ZO-1**) was reduced in Dox-treated human cardiac ECs, increasing the Dox access and exposure time to the myocardium (Wilkinson et al., 2016). How Dox decreases the expression of ZO-1 is unknown, though the loss of ECs and increased dysfunction can act to increase the permeability of the endothelial defence.

Furthermore, the role of BRCA2 in the endothelium has not been explored, and it presents a novel opportunity to investigate if dysfunctional BRCA2 results in a dysfunctional/vulnerable endothelium, which may promote the access of agents such as Dox to cardiomyocytes. The endothelium is susceptible to exacerbated damage with the administration of Dox, as Dox promotes DNA damage in all cells and results in the accumulation of TNFα, ROS, and the inhibition of eNOS (He et al., 2020; Wolf & Baynes, 2006). Subsequently, the mechanisms of Dox toxicity and the loss of BRCA2 are similar, and thus, together, may exacerbate cellular dysfunction and death (compare **Figures 1 and 2**). Together, these factors rationalize a comprehensive evaluation of endothelial BRCA2 in loss-of-function models with Dox.

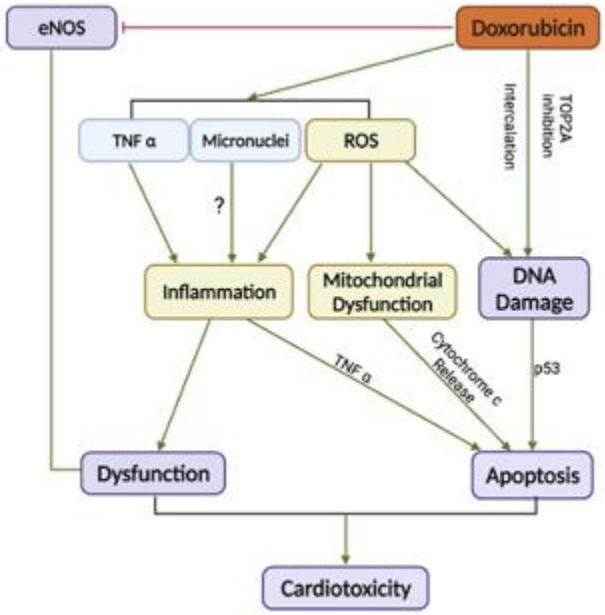

Figure 2. Schematic depicting the mechanistic role of Dox in cardiotoxicity.

2 RATIONALE, HYPOTHESIS AND OBJECTIVES

2.1 Rationale

Singh et al. reported that Dox treatment in cardiomyocyte-specific *BRCA2* knockdown mice resulted in exacerbated p53-mediated cardiomyocyte apoptosis leading to increased cardiac dysfunction (K. K. Singh et al., 2012). So far, previous research has been focused mainly on cardiomyocyte toxicity, but the focus has recently shifted to understanding the role of the endothelium in Dox-induced cardiotoxicity (Luu et al., 2018). Dox is delivered systemically, where endothelial cells are the first line of contact, as they form the innermost cell layer in the lumen of blood vessels. Furthermore, Dox must first infiltrate through the endothelium to exert its effects on cardiomyocytes (Mitry & Edwards, 2016). Previously, it was demonstrated that Dox treatment and increased oxidative stress (Singh et al., 2020) can induce endotheliotoxicity in human umbilical vein endothelial cells (**HUVECs**) *in vitro*. Therefore, Dox-induced endotheliotoxicity in cardiac endothelial cells is expected to enhance drug access to cardiac tissue and promote cardiomyocyte death/dysfunction leading to heart failure in severe cases.

2.2 Hypothesis

We hypothesized that endothelial-specific loss of *BRCA2* will induce doxorubicin-induced endothelial dysfunction and exacerbate DIC.

2.3 Objectives

Our first objective was to investigate the changes in the cardiac molecular profile and heart function following Dox treatment in endothelial cell-specific *BRCA2* knockdown mice. Our second objective was to characterize the effects of Dox treatment on HUVEC and human coronary arterial endothelial cell (**HCAEC**) apoptosis, proliferation, and tube formation *in vitro*.

3 METHODS

3.1 Animal Studies

All animal studies were approved by Western University's Animal Care. All animal procedures were performed following guidelines provided by the Canadian Council on Animal Care. Experiments were performed on male and female C57BL/6J mice aged 8 to 16 weeks, housed in a controlled sterile environment on a 12 h light/dark cycle. Mice were supplied with a reverse osmosis water chow-type diet (NIH-31, Cat# 7013, Open Formula Mouse/Rat diet, irradiated – Envigo) *ad libitum*.

Doxorubicin hydrochloride (Sigma-Aldrich, Cat # 25316-40-9) was dissolved in sterile 0.9% saline solution (NaCl) for a final dose of 10 or 20 mg/kg and injected intraperitoneally (**IP**) in a sterile environment (Amin et al., 2023; Chen et al., 2015; Gomes-Santos et al., 2021; Krishnamurthy et al., 2015; V. Z. Luu et al., 2020; K. K. Singh et al., 2012; S. Singh et al., 2020). Vehicle-treated mice were injected with sterile 0.9% saline IP. Mice were monitored daily for morbidity and mortality and were weighed at baseline before injections, and 7 days post-administration.

3.2 Generation of Endothelial-Specific *BRCA2* Knockdown Mice

Endothelial cell-specific *BRCA2* knockdown mice were generated using the Cre-LoxP system of tissue-specific gene excision (K. K. Singh et al., 2012). Mice homozygous for the exon 11 floxed *BRCA2* allele with a BALB/cJ background (NCI; Strain #: 01XB9; Common name: *BRCA2* floxed; Strain Nomenclature: STOCK *BRCA2*tm1Brn/Nci) were crossed with mice hemizygous for Cre-recombinase expression under the control of the vascular endothelial Cadherin 5 promoter and on a C57BL/6J background (The Jackson Laboratory; Stock #: 006137; Common Name: VE-

Cadherin-Cre (VE-CRE; Strain Nomenclature: B6.FVB-Tg(Cdh5-cre)7Mlia/J). Mice were bred based on the pairing described in **Figure 4A** to generate VE-Cre: *BRCA2*fl/fl; VE-CreTg/+ (**BRCA2^{endo}**) and heterozygote knockdown BRCA2fl/wt; VE-CreTg/+ (**BRCA2^{het}**) mice. BRCA2fl/fl; VE-Cre+/+ and BRCA2fl/wt; VE-Cre+/+ and BRCA2wt/wt; VE-CreTg/+ (**BRCA2^{WT}**) were used as control wildtype (**WT**) mice.

3.3 Echocardiography

Two-dimensional echocardiography (VisualSonics Vevo 2100 imaging system) was performed on anaesthetized mice (4% induction, 1.5-2% maintenance with isoflurane) who had their chests shaved and residual hair removed with Nair (Imaging Facility, Robarts). B-Mode was used to identify the mid-papillary muscle whereby M-Mode was utilized for mono-dimensional images. Three intervals were used to capture systole and diastole and the left ventricular (**LV**) end-systolic dimension (**LVESC**) and left ventricular end-diastolic dimension (**LVEDD**) were measured. LV fractional shortening (LVFS) was calculated as (LVEDD - LVESC)/LVEDD), and LV ejection fraction (**LVEF**) was calculated as ((LVEDD3-LVESC3)/LVEDD3) x 100).

3.4 Tissue Collection

Mice were placed under deep anesthesia using the bell jar isoflurane method. Incisions were made into the parietal peritoneum and further cuts were made along the ribcage to access the thoracic cavity. The heart was exsanguinated via right ventricle cardiac puncture using a 27-gauge needle. Heart, aorta, and lung tissues were collected on dry ice and either snap-frozen and stored at -80°C for molecular analyses or placed in 10% formalin and stored at 4°C for histology.

3.5 Tissue Histology

Formalin-fixed heart tissues were processed by undergoing a typical dehydration sequence and

cleared in Xylene. The tissues were infiltrated with paraffin wax and embedded in tissue sectioning blocks. A microtome was then used to section the left ventricle of the hearts at 5 µm and sections were mounted onto plus-charged microscope slides.

Heart tissues were stained with either a routine Hematoxylin & Eosin (**H&E**) via autostainer or picrosirius red (**PR**) using a Picro Sirius Red Stain Kit with the manufacturer's protocol (Abcam, Cat # ab150681). The tissues were then dehydrated, and cover slipped using resinous mounting media. Whole microscope slide scans were completed using a microscope slide auto scanner. Histology was performed at Robarts Imaging Facility.

3.6 HUVECs and HCAECs Culture

The human umbilical vein or human coronary artery endothelial cells (HUVECs or HCAECs, pooled, Lonza; passage 4–6) were cultured in complete endothelial cell growth medium-2 (EGM-2 Bulletkit; Lonza) supplemented with human epidermal growth factor, hydrocortisone, GA-1000, ascorbic acid, bovine brain extract, and 2% fetal bovine serum at 37°C in humidified 5% CO_2. siRNA-mediated *BRCA2* gene knockdown was performed with si*BRCA2* or scrambled control per the manufacturer's guidelines (DharmaconTM). A standard reverse transfection reagent (Lipofectamine ® 3000, Invitrogen), and 5 nm si*BRCA2* (DharmaconTM, Cat # A-003462-13-0005) or scrambled control (DharmaconTM, Cat # 2575450) were used. RNA or protein was collected using Trizol reagent (Invitrogen) or RIPA buffer, respectively, following 48 post-transfection and incubation with Dox or vehicle control for 20 h. Cells were treated with doxorubicin hydrochloride (Sigma-Aldrich, Cat # 25316-40-9) dissolved in dimethyl sulfoxide (**DMSO**) to achieve Dox doses of 0, 1, 2.5, and 5 µM (Lorenzo et al., 2002; Maestre et al., 2001). Control groups were treated with DMSO.

3.7 Cell Counting and WST-1 Absorbance

HUVECs were knocked down for *BRCA2* and seeded at a density of 2×10^5 cells/well in a 6-well plate before Dox or vehicle control (DMSO) for 24 h. Cells from each well were then harvested and counted under an Automated Cell Counter (CytoSmart) to assess cell viability.

HCAECs were silenced and seeded at a density of 1.5 x104 cells/well in a 96-well plate, then treated with Dox or vehicle diluent for 24 h. The manufacturer's protocol for the WST-1 Cell Proliferation Kit (Abcam, Cat # ab155902) was followed for proliferative measurements. 10 µL of WST Solution was added to each well, being careful not to introduce any bubbles to the wells and protect them from light. Following 1 hour of incubation at 37°C (in humidified 5% CO2), the plate was shaken thoroughly for 1 minute and absorbance at 480 nm was measured using a microtiter plate reader (BioRad).

3.8 Migration Assay

HUVECs or HCAECs were initially seeded and grown to 80% confluency in 60 mm dishes and silenced for *BRCA2* via reverse transfection. These cells were then seeded at a density of 2 × 105 cells/well in a 6-well plate and grown to 70-80% confluency in a complete medium. A 200 µL tip was used to administer a scratch in each well before Dox or negative control treatment. Wells were washed with PBS and a low-serum (1% FBS) MCDB-131 media was added with 2.5 µM Dox or vehicle control (DMSO). Phase-contrast microscopy using an adapted camera (Optika) was employed to take pictures of cells in each well migrating into the scratch at baseline, 8 h, and 20 h to evaluate for migrating capacity as described (Jonkman et al., 2014). Each experiment was performed in triplicates.

3.9 Tube formation assay

The In vitro Angiogenesis Kit (Millipore) was employed to evaluate endothelial tubule formation. HUVECs were transfected and seeded at a density of 2 × 105 cells/well in a 6-well plate and allowed to grow to ~75% confluency. The kit-provided matrix solution was added into designated wells of a 96-well plate. Transfected cells were then harvested and seeded at an equal density of 1 to 1.5 × 104 cells/well onto the designated wells in EGM-2 media supplemented with Dox or vehicle diluent (DMSO). Phase contrast microscopy was employed (Optika) to obtain photomicrographs in each designated well at baseline and 4 h to monitor tube formation. Quantification was performed on ImageJ by assessing the mesh area.

3.10 RNA Extraction, cDNA Synthesis and qPCR

Total RNA from cultured endothelial cells and harvested heart tissues were extracted using Trizol reagent (Invitrogen) into 1 mL DNase/RNase-free Eppendorf tubes and allowed to incubate at room temperature for 5-10 minutes. Phase separation was observed by adding 200 µL of chloroform and shaking vigorously for 15 seconds. After incubating at room temperature for 3 minutes, the Eppendorf tubes were centrifuged at 12,000 RCF and 4°C for 15 minutes. 400 µL of the clear, upper RNA phase was transferred to a new set of labelled Eppendorf tubes. RNA was precipitated by adding 500 µL of isopropyl alcohol and inverting 10 times before incubating for 10 minutes at room temperature. The Eppendorf tubes were then centrifuged at 12,000 RCF at 4°C for 10 minutes to pellet the RNA. The supernatant was poured off being careful not to disturb the pellet and 1mL of 75% ethanol was added to wash the pellet by first lightly vortexing to wash the pellet before centrifuging at 7,500 RCF at 4°C for 5 minutes. This step was repeated once more. The ethanol was then poured out and the pellet was allowed to air dry for 5-10 minutes. The RNA pellet was then dissolved in 20 µL of sterile water, reconstituted with a pipette, and vortexed before a 3-minute incubation period at 65°C. The Eppendorf tubes were then immediately placed on ice

to proceed with complementary DNA (**cDNA**) synthesis. cDNA synthesis was performed using QIAGEN's QuantiTect reverse transcription kit (Cat# 205311) using 1µg RNA/sample and an Eppendorf PCR Mastercycler.

Quantitative polymerase chain reaction (**qPCR**) was performed with SYBR Select Master Mix (Applied Biosystems) on the Quantstudio 3TM with the standard protocol using primers forward and reverse primers for *BRCA2, BNP, alpha myosin heavy chain* (***aMHC***), *beta myosin heavy chain* (***bMHC***), and *fatty acid binding protein-3* (***FABP3***), and *glyceraldehyde 3-phosphate dehydrogenase* (***GAPDH***) (S. Singh et al., 2020). PCR reactions were prepared using 5µL SYBR, 0.5µM final concentration of forward and reverse primers, 2-3µL cDNA, and balanced to 10 µL with sterile water. Each combination was performed in triplicates and fold-change expression was calculated by the Delta Delta CT method.

3.11 Immunoblotting

Cultured HUVECs or heart tissues were collected in RIPA buffer to isolate total proteins (Subedi et al., 2019). An equal amount of total protein (30 µg) from each sample was loaded onto sodium dodecyl sulfate-polyacrylamide gels and subjected to electrophoresis. Proteins were then transferred onto PVDF membranes (Bio-Rad), and the following antibodies were employed to detect the proteins of interest: [Cell Signaling Technology: BRCA2 (#9012, dilution 1:1000), p53 (#9282, dilution 1:1000), and GAPDH (#5174S, dilution 1:1000)]. Western blots were developed using chemiluminescence substrates (Bio-Rad) and the Licor-Odyssey XF Imaging System. Densitometry was performed to measure the band intensities using the Image Studio Lite.

3.12 Data and statistical analyses

Survival data were analyzed by the Log-rank test using survival curve analysis. Otherwise, the difference between the means of two groups and more than two groups was calculated using an

unpaired t-test and analysis of variance (**ANOVA**) statistical analyses, respectively. ANOVA significant results were followed by the post hoc Tukey's test. Data are presented as mean ± SD unless otherwise indicated. N = number of independent experiments or animals. For cardiomyocyte area calculations, 3 technical replicates (20x images) were taken, and 20 cardiomyocytes/images were highlighted using the polygon tool on ImageJ. For fibrosis % area coverage calculations, 3 technical replicates (1.6x images, with each image being a transverse section of the LV) were taken. Total sectional Sirius red coverage was calculated by taking the percent area of heart sections.

4 RESULTS

4.1 Evaluating endothelial cell-specific loss of *BRCA2* on Dox-induced cardiotoxicity *in vivo*

4.1.1 Dox induced *BRCA2* expression in the heart of wild-type mice

Wild-type C57BL/6J mice from the age range of 8 to 12 weeks were IP injected with vehicle (0.9 % sterile saline) or Dox (20 mg/kg) and euthanized after 7 days. Heart tissues were collected, the left ventricle was isolated, and RNAs were extracted. Subsequently, cDNA synthesis and qPCR were performed to examine for *BRCA2* transcript levels. The data shows that mice administered Dox had higher expression levels of *BRCA2* than vehicle-treated wild-type mice (**Figure 3**).

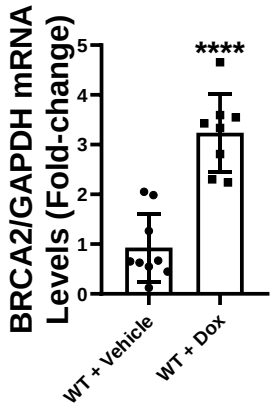

Figure 3. Dox administration induced *BRCA2* expression in the heart of wild-type mice. Dox administration induced *BRCA2* expression in the heart of wild-type mice. WT mice treated with 20mg/kg of Dox showed increased expression of *BRCA2* mRNA in the heart 7 days post-administration compared to vehicle-treated controls. Data presented as mean +/-SD. **** indicates statistical significance $p<0.0001$ vs. WT + Vehicle, unpaired t-test, n=8-9 per group, 8-10 weeks old males.

4.1.2 Generation and characterization of EC-specific *BRCA2* knockdown (BRCA2^{endo}) mice

Our lab has previously generated and characterized BRCA2^{endo} mice generated using the Cre-LoxP system (**Figure 4B**). Briefly, mice homozygous for the exon 11 floxed BRCA2 allele with a BALB/cJ background (NCI; Strain #: 01XB9; Common name: BRCA2 floxed; Strain Nomenclature: STOCK BRCA2tm1Brn/Nci) were crossed with mice hemizygous for Cre-recombinase expression under control of the vascular endothelial (VE) Cadherin 5 promoter and on a C57BL/6J background (The Jackson Laboratory; Stock #: 006137; Common Name: VE-Cadherin-Cre (VE-CRE; Strain Nomenclature: B6.FVB-Tg(Cdh5-cre)7Mlia/J). Breeding was performed following the schematic in **Figure 4A**. Mice were bred to generate EC-specific BRCA2 heterozygous and homozygous [heterozygote knockdown *BRCA2*fl/wt; VE-Cretg/- (**BRCA2^{het}**); homozygote knockdown VE-Cre: *BRCA2*fl/fl; VE-Cretg/- (**BRCA2^{endo}**)] knockdown mice. Wildtype littermates – *BRCA2*fl/fl;VE-Cre-/-, *BRCA2*fl/wt;VE-Cre-/- and *BRCA2*wt/wt;VE-Cretg/-– were used as wild-type littermate controls (**BRCA2^{WT}**). Successful EC-specific deletion was confirmed at transcript and protein levels specifically in endothelial cells (**Figure 4C, D**).

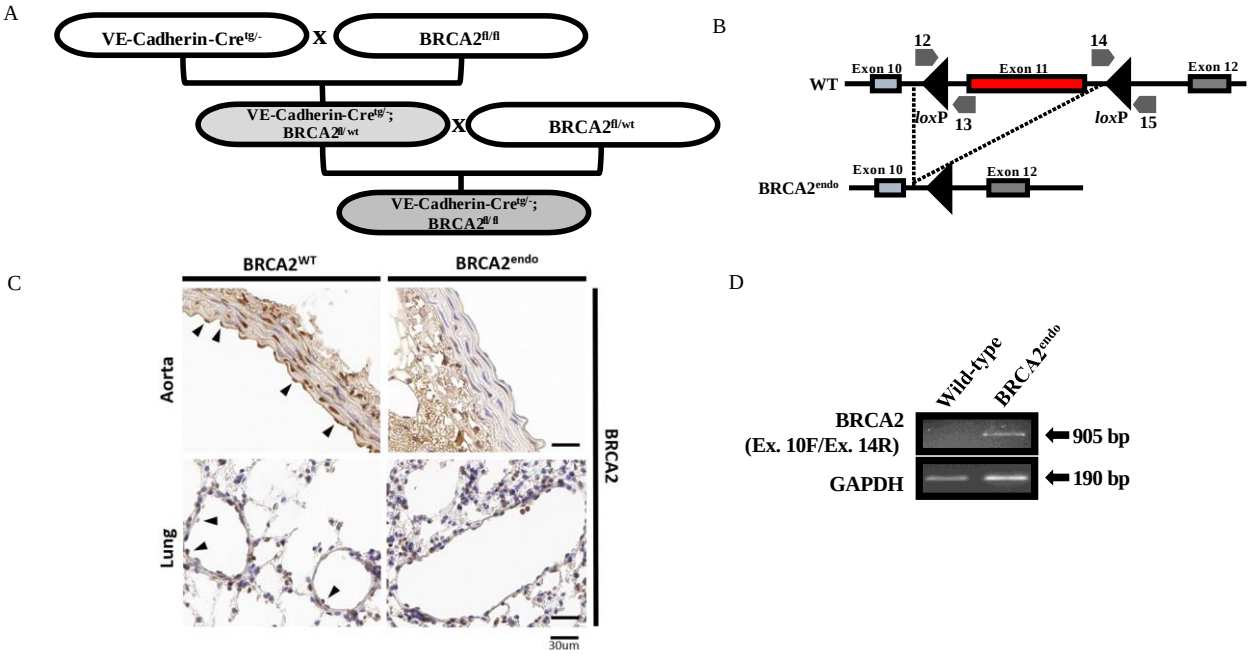

Figure 4. The generation and characterization of EC-specific BRCA2^{endo} mice. The (A) breeding strategy using the (B) Cre-Lox P system in the generation of the EC-specific *BRCA2* knockdown mice. (C) Lung and aortic tissue showed the successful deletion of BRCA2 in ECs. (D) Aortic ECs were extracted, RNA was isolated, cDNA was synthesized, and qPCR for exon 10 forward and exon 14 was performed. A deleted 905 kb product was only present in knockdown mouse tissue. Scale bar = 30 µm, n=3 per group, 8-10 weeks old male mice (Michels et al., *unpublished*).

4.1.3 BRCA2^{endo} mice demonstrated augmented weight loss following Dox treatment

Male and female EC-specific BRCA2^{endo} mice did not show changes in weight at baseline or following vehicle administration (**Figures 5A, B**). However, both male and female EC-specific BRCA2^{het} and BRCA2^{endo} mice showed significant weight loss following 10 mg/kg Dox administration after 7 days compared to Dox-treated WT mice (**Figures 5C, D**). We utilized a lower dose of Dox (10 mg/kg), which is in line with previous reports (K. K. Singh et al., 2012) to ensure sufficient survival of mice for subsequent functional and molecular analyses.

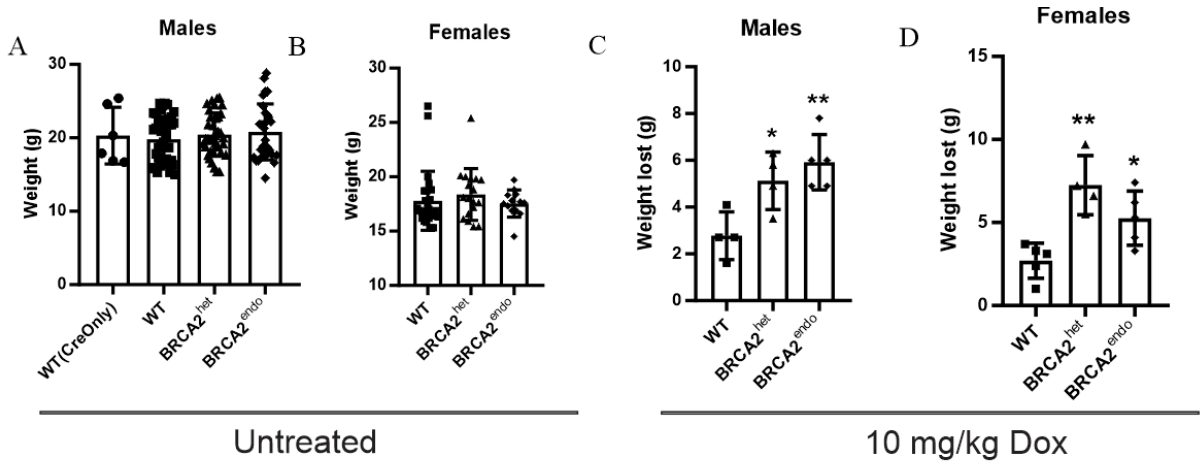

Figure 5. Mice with EC-specific loss of *BRCA2* showed increased weight loss following 10 mg/kg Dox treatment. BRCA2endo, BRCA2het, and WT mice showed similar weight at baseline in both (A) male and (B) female mice. 7 days post-administration of 10 mg/kg Dox, (C) male and (D) female heterozygous (BRCA2^{het}) and homozygous (BRCA2^{endo}) mice showed increased weight loss compared to Dox-treated WT mice. Data presented as mean +/-SD.

*, ** indicates statistical significance, p<0.05, p<0.01 vs. WT + Dox respectively, one-way ANOVA, n=6-44 per group, 8-10 weeks-old male and female mice.

4.1.4 EC-specific loss of *BRCA2* promoted Dox-induced cardiac dysfunction

At baseline, echocardiography was performed on 8-16 weeks old male and female mice who did not show any sign of cardiac dysfunction as measured by LVEF or LVFS (**Figure 6A-D**).

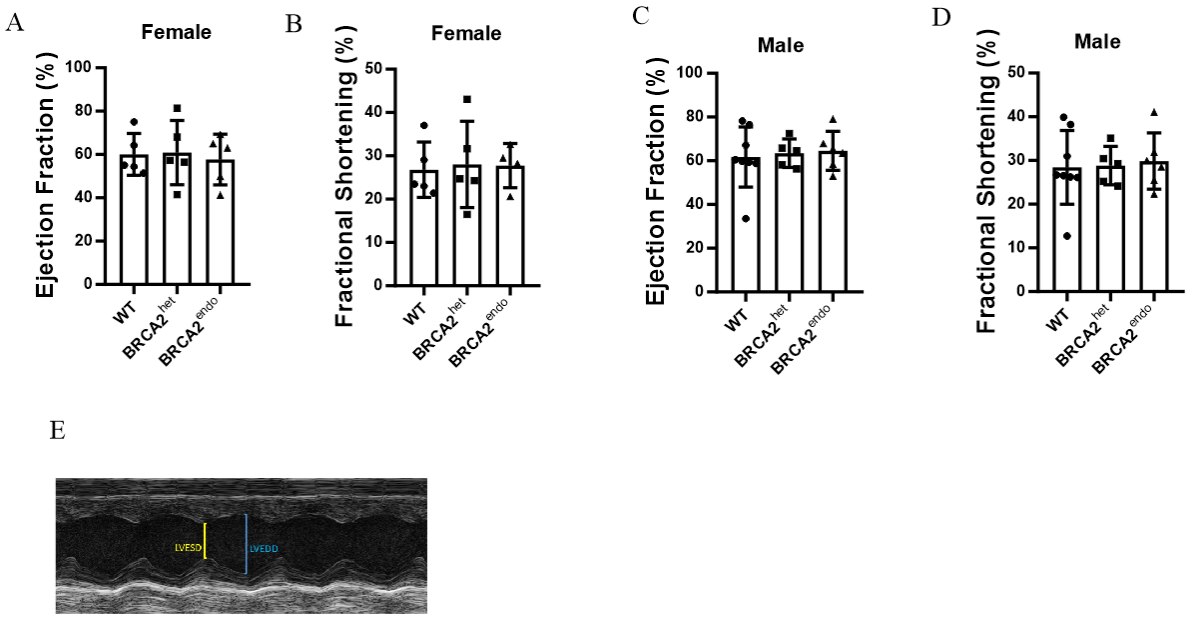

Figure 6. Baseline echocardiography show similar cardiac function in BRCA2^{endo}, BRCA2^{het} and WT mice. (A, B) Female and (C, D) male heterozygous (BRCA2^{het}) and homozygous (BRCA2^{endo}) mice do not show differences in cardiac function assessed via echocardiography presented as left-ventricular ejection fraction (A, C) and fractional shortening (B, D). Data presented as mean +/-SD, one-way ANOVA, n=6-7 per group, 8-16 weeks-old male and female mice (Michels et al, *unpublished*).

However, significant cardiac dysfunction occurred in EC-specific BRCA2 knockdown mice after administration of 10 mg/kg Dox. Echocardiography was performed to assess LVEF and LVFS. In support of our hypothesis, BRCA2endo mice demonstrated a significant decrease in LVEF (Figure

7A, B) and LVFS (Figure 7C, D) compared to Dox-treated WT mice.

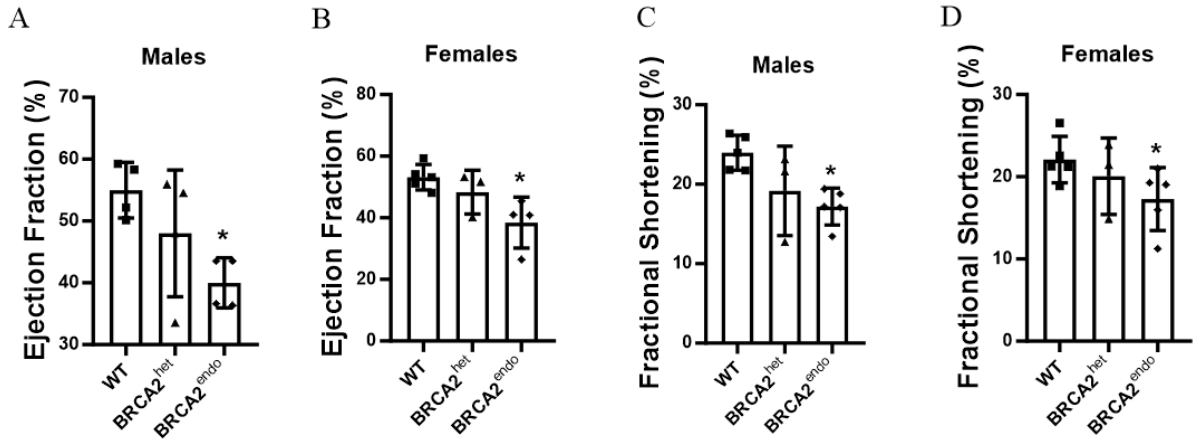

Figure 7. Significant cardiac dysfunction in EC-specific *BRCA2* knockdown mice treated with 10 mg/kg Dox. Echocardiography performed 7 days post-dox administration in EC-specific BRCA2 knockdown mice show reduced ejection fraction and fractional shortening in both males (A, C respectively) and females (B, D respectively) in homozygous mice compared to Dox-treated WT mice. Data presented as mean +/- SD. * indicates statistical significance, $p<0.05$ vs. WT, one-way ANOVA, n=6-7 per group, 8-10 weeks old male and female mice.

4.1.5 EC-specific loss of *BRCA2* upregulated markers of heart failure in Dox-treated mice

Seven days following the administration of 10 mg/kg Dox or vehicle, heart tissues were collected, the left ventricle was isolated, and RNA was extracted from mechanically lysed tissue using Trizol. cDNA synthesis and qPCR were performed to examine the expression levels of the heart failure markers *BNP*. Mice administered Dox showed significantly higher expression levels of *BNP* compared to vehicle-treated mice, independent of *BRCA2* expression status. Additionally, apart from *BNP*, all other markers were further elevated in Dox-treated BRCA2^{endo} mice compared to Dox-treated WT mice (**Figure 8A-D**).

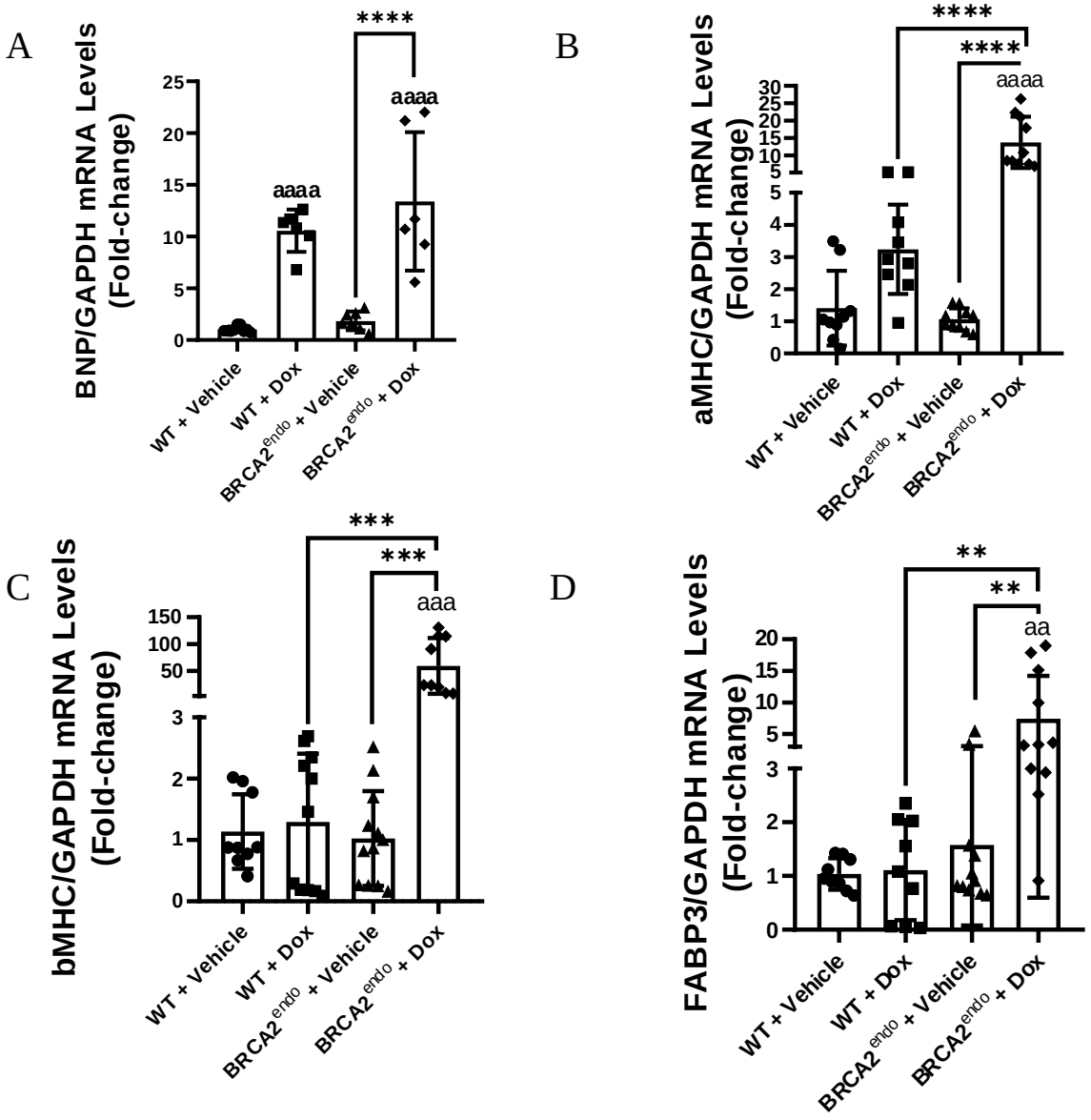

Figure 8. EC-specific loss of *BRCA2* upregulated markers of heart failure in Dox-treated mice. Seven days post-administration of 10 mg/kg Dox, EC-specific *BRCA2* knockdown male homozygous (BRCA2^{endo}) mice show differences in (A) BNP, (B) aMHC, (C) bMHC, and (D) FABP3. aa, aaa, aaaa indicates statistical significance vs. WT + Vehicle, $p<0.05$, 0.001, 0.0001 respectively; **, ***, **** indicates statistical significance, $p<0.01$, 0.001, 0.0001 respectively. Data presented as mean +/- SD, one-way ANOVA, n=4-5 in triplicates per group, 8-10 weeks old male mice.

4.1.6 Dox treatment significantly increased cardiomyocyte hypertrophy in BRCA2^{endo} mice

Seven days following the administration of 10 mg/kg Dox, heart tissues were collected, the left ventricle was isolated, fixed in paraffin and sectioned onto microscope slides for H&E staining (**Figure 9A**). Cardiomyocyte cross-sectional areas were calculated by outlining the cells with clear nuclei and recording the values by ImageJ. In the male mice, only BRCA2^{het} mice treated with dox exhibited significant increase in cardiomyocyte area compared to vehicle-treated WT and BRCA2^{het} mice. In females, Dox-treated BRCA2^{endo} mice had significantly increased cardiomyocyte area compared to vehicle-treated WT mice; however, only Dox-treated BRCA2^{het} mice showed significant increase in cardiomyocyte area compared to their vehicle-treated BRCA2^{het} mice littermates (**Figure 9B, C**).

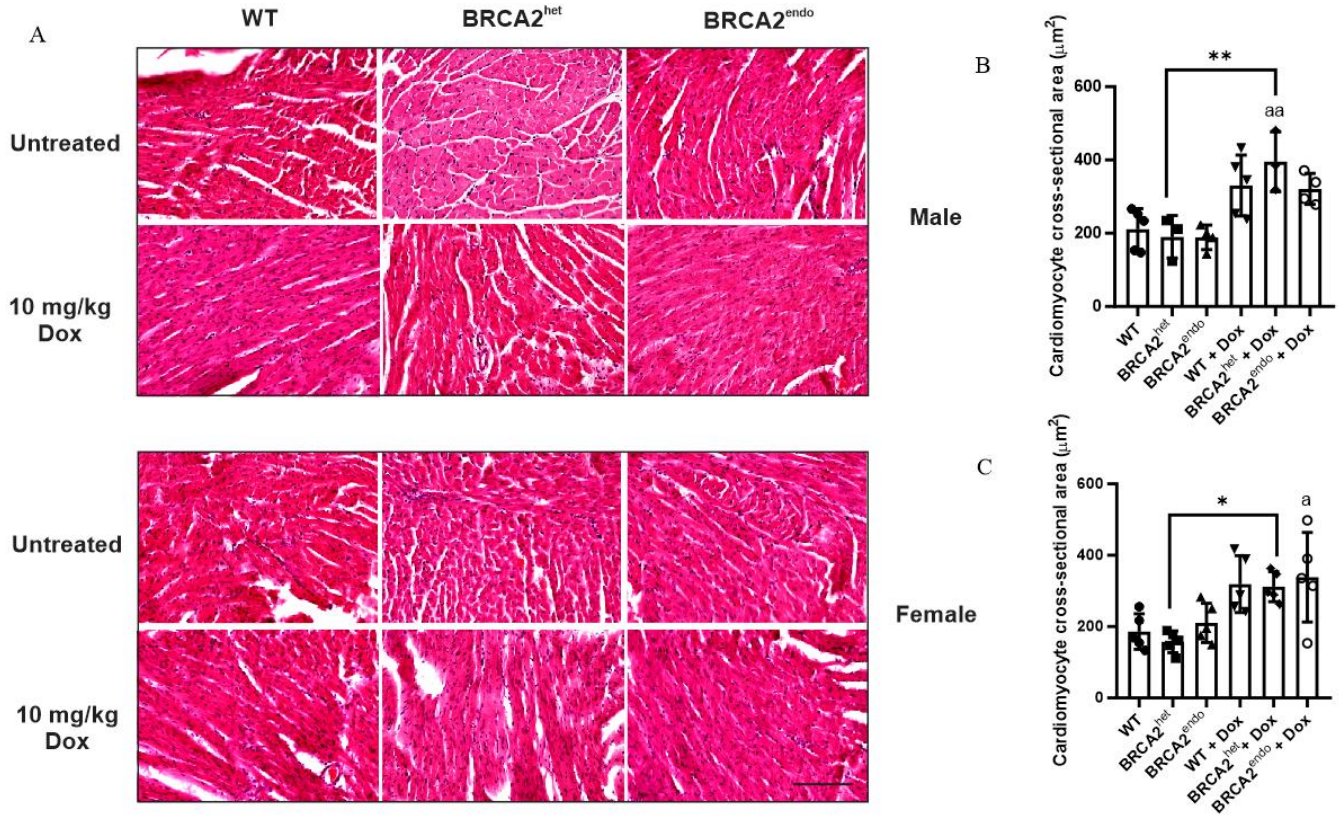

Figure 9. Dox treatment significantly increases cardiomyocyte hypertrophy in the hearts of BRCA2^{endo} mice.

(A) Heart sections (5 μm) stained for H&E in EC-specific *BRCA2* knockdown mice treated with 10 mg/kg Dox to

demonstrate changes in cardiomyocyte area vs. vehicle-treated WT mice. Scale bar = 1 mm Quantification of (B) male and (C) female cardiomyocyte cross-sectional area in μm^2. Male and female $BRCA2^{het}$ mice treated with Dox show increased cardiomyocyte area compared to their vehicle-treated littermates. Data presented as mean +/- SD. a, aa indicates statistical significance vs. WT, $p<0.05$, 0.01 respectively; *, ** indicates statistical significance, $p<0.05$, 0.01 respectively, one-way ANOVA, n=3-5 per group, 8-10 weeks old male and female mice.

4.1.7 Dox treatment significantly increased cardiac fibrosis in mice with EC-specific loss of *BRCA2*

Seven days following the administration of 10 mg/kg Dox, heart tissues were collected, the left ventricle was isolated, and fixed in paraffin and sectioned onto microscope slides and stained with Picrosirius Red to assess cardiac fibrosis, which is one of the major contributors of cardiac dysfunction (**Figure 10A**). Cardiac fibrosis was measured via threshold analysis on ImageJ, wherein the % area coverage of collagen-stained Sirius red was calculated against picric-stained cardiac tissue. Both males and female mice administered with 10 mg/kg Dox displayed significant increase in the percentage of collagen area coverage compared to the vehicle-treated WT mice. Additionally, both male and female $BRCA2^{het}$ and $BRCA2^{endo}$ mice administered with 10 mg/kg Dox showed increased fibrosis compared to their vehicle-treated littermates (**Figure 10B, C**).

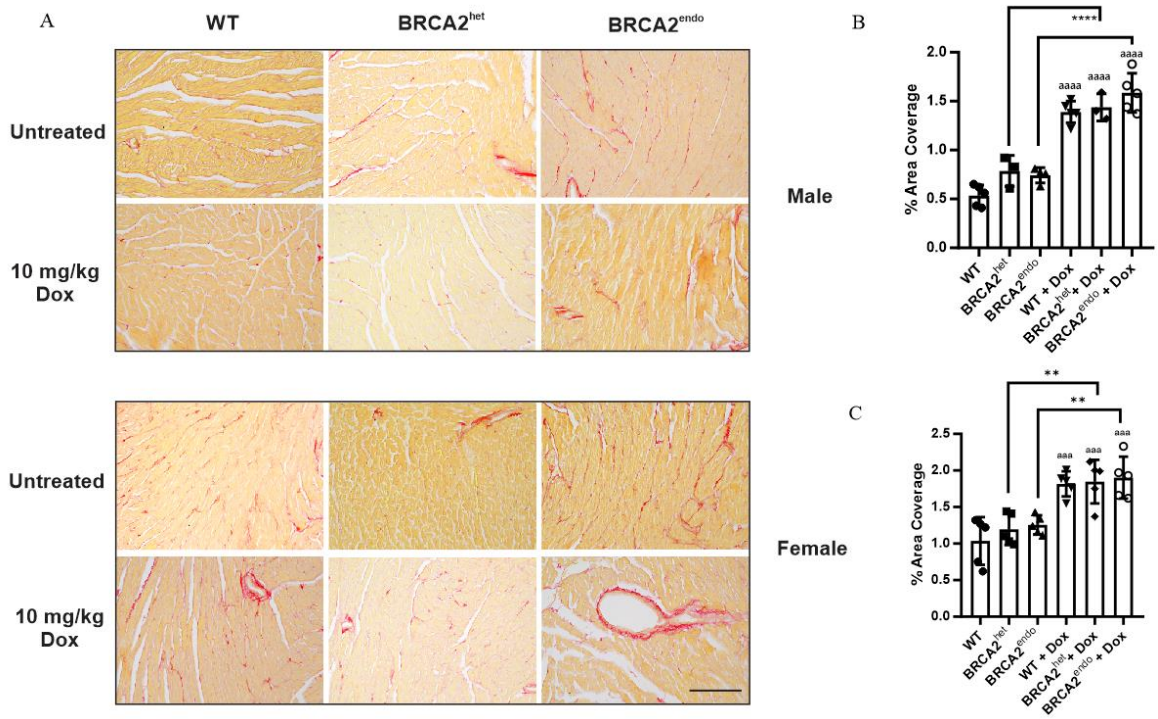

Figure 10. Dox treatment significantly increases fibrosis in the hearts of mice with EC-specific loss of *BRCA2*. (A) Heart sections (5 µm) stained for picrosirius red in EC-specific *BRCA2* knockdown mice treated with 10 mg/kg Dox to demonstrate changes in collagen deposition vs. saline-treated WT. Scale bar = 1 mm. Quantification of (B) male and (C) female cardiac fibrosis in % area coverage of picrosirius red. Data presented as mean +/- SD. aaa, aaaa indicates statistical significance vs. WT, p<0.001, 0.0001 respectively; **, ***, **** indicates statistical significance, p<0.01, 0.001, 0.0001 respectively, one-way ANOVA, n=3-5 per group, 8-10 weeks old male and female mice.

4.1.8 EC-specific loss of *BRCA2* increased Dox-induced mortality

Having utilized a lower dose of Dox to assess the functional and structural cardiovascular implications of Dox administration, we did not see any significant difference in mortality in Dox-treated mice compared to vehicle-treated mice. As heart failure is a fatal outcome in clinic, we wanted to investigate dox-induced mortality in our mice. The Dox dose was increased to 20 mg/kg based on increased mortality demonstrated by our group in cardiomyocyte-specific *BRCA2* knockdown mice (K. K. Singh et al., 2012). We observed increased mortality across all groups, which was further exacerbated by endothelial cell-specific loss of *BRCA2* (**Figure 11**).

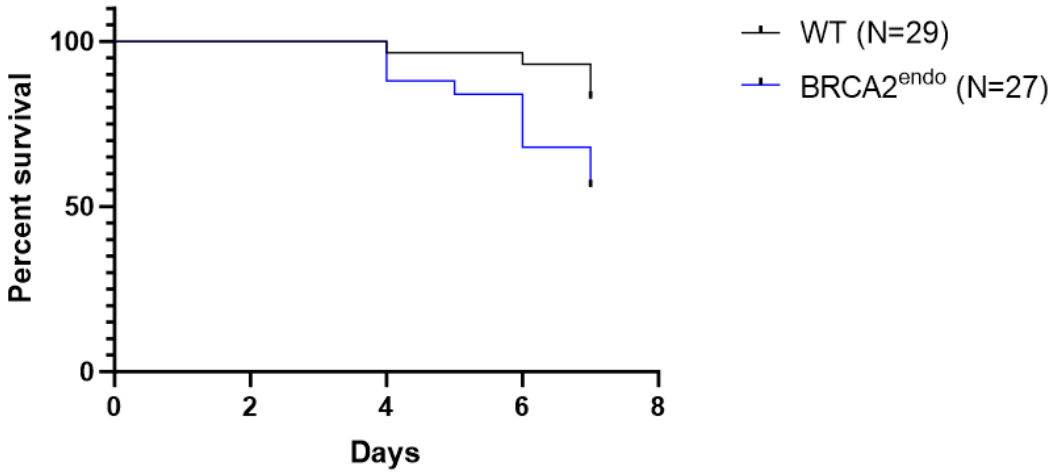

Figure 11. EC-specific loss of *BRCA2* promotes Dox-induced mortality. After 7 days post-administration of 20 mg/kg Dox, EC-specific *BRCA2* knockdown male and female homozygous mice show increased mortality compared to vehicle treated WT mice. Data presented as mean +/- SD. Survival curve analysis with Log-rank test yielded $p<0.05$. n=29 for WT and n=27 for Homozygous, 8-10 weeks old male and female mice.

4.1.9 Mice with EC-specific loss of *BRCA2* showed increased weight loss and cardiac dysfunction following treatment with 20 mg/kg Dox

Male BRCA2^{endo} mice showed significantly higher weight loss following 20 mg/kg Dox administration after 7 days compared to Dox-treated WT littermates (**Figure 12A, B**). Male BRCA2^{het} and BRCA2^{endo} mice administered with 20 mg/kg Dox show decreased LVEF (**Figure 12C**) and LVFS (**Figure 12D**) compared to Dox-treated WT mice.

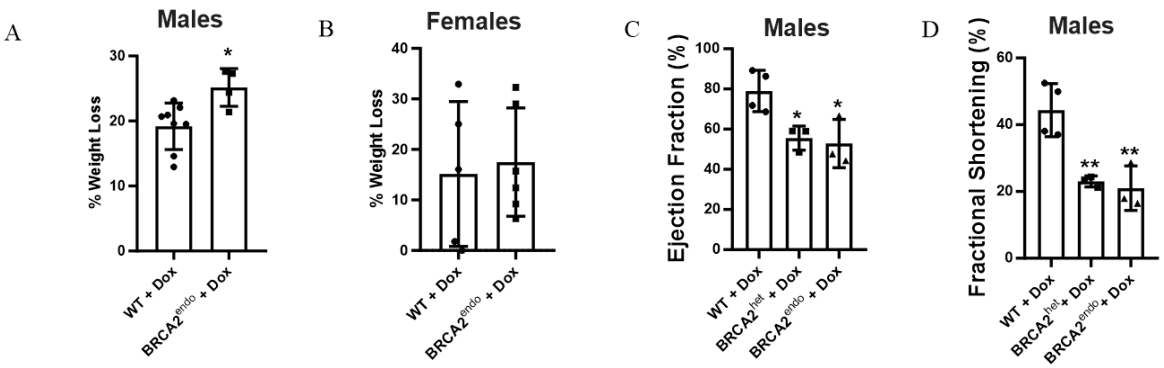

Figure 12. Mice with EC-specific loss of *BRCA2* show increased weight loss and cardiac dysfunction following treatment with 20 mg/kg Dox. 7 days post-administration of 20 mg/kg Dox, EC-specific *BRCA2* knockdown (A) male, but not (B) female homozygous ($BRCA2^{endo}$), mice show increased weight loss compared to WT + Dox mice. Echocardiography performed 7 days post-Dox administration in EC-specific *BRCA2* knockdown mice show reduced ejection fraction (C) and fractional shortening (D) in male homozygous and heterozygous mice compared to WT + Dox mice. Data presented as mean +/- SD. *, ** indicates statistical significance, $p<0.05$, $p<0.01$ vs. WT respectively, unpaired t-test (A, B) or one-way ANOVA (C, D), n=3-7 per group, 8-10 weeks old male and female mice.

4.1.10 Higher Dox dose increased cardiomyocyte hypertrophy in EC-specific *BRCA2* knockdown mice

Seven days following the administration of 20 mg/kg Dox, heart issues were collected, the left ventricle isolated and mounted in paraffin and sectioned onto microscope slides and stained with H&E (**Figure 13A**). Cardiomyocyte cross-sectional areas were calculated by outlining cells with clear nuclei and recording area values generated by ImageJ. In male mice, only WT mice treated with 20 mg/kg exhibited significant increase in cardiomyocyte area compared to vehicle treated WT mice. $BRCA2^{endo}$ mice administered with 20 mg/kg Dox also showed increased cardiomyocyte area compared to their vehicle-treated counterparts (**Figure 13B**). In females, no significant difference in cardiomyocyte areas were observed (**Figure 13C**).

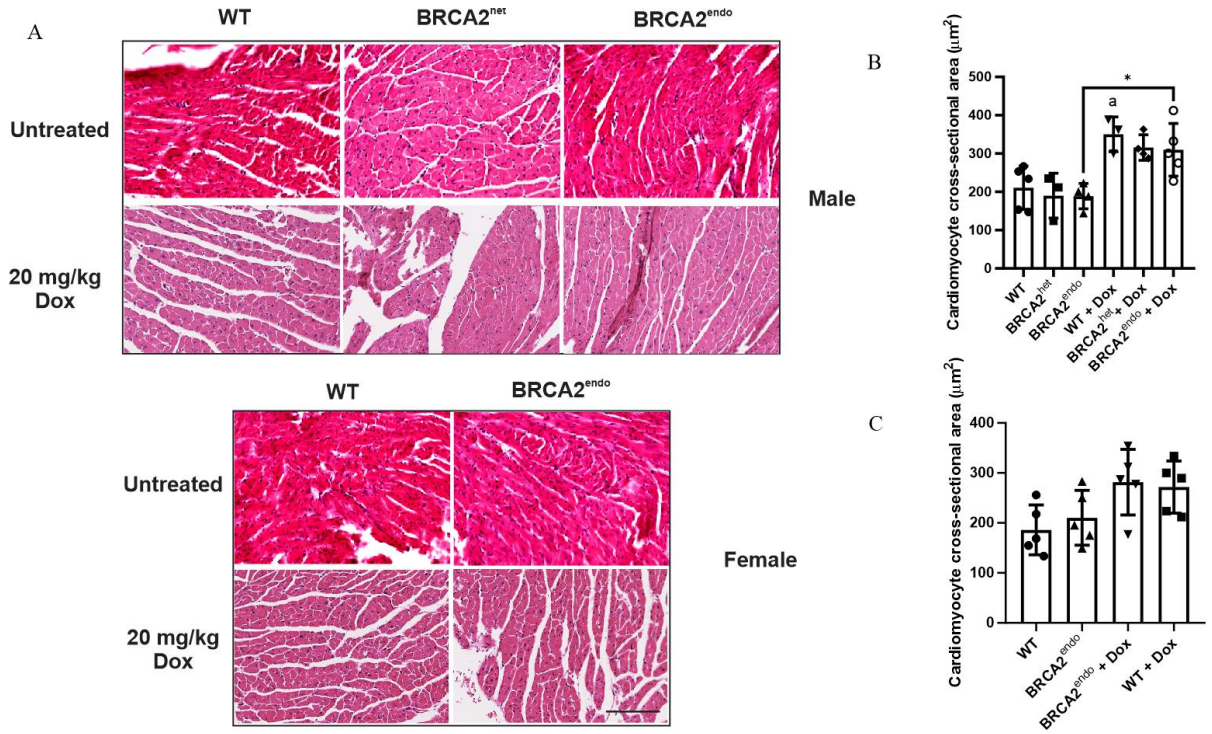

Figure 13. Higher Dox dose significantly increases cardiomyocyte hypertrophy in the hearts of BR EC-specific *BRCA2* knockdown mice. (A) Heart sections (5 µm) stained for H&E in EC-specific *BRCA2* knockdown mice treated with 20 mg/kg Dox to demonstrate changes in cardiomyocyte area vs. untreated WT mice. Scale bar = 1 mm Quantification of (B) male and (C) female cardiomyocyte cross-sectional area in μm^2. Data presented as mean +/- SD. a indicates statistical significance vs. WT, $p<0.05$; * indicates statistical significance, $p<0.05$, one-way ANOVA, n=3-5 per group, 8-10 weeks old male and female mice.

4.1.11 Higher Dox dose increased fibrosis in the hearts of EC-specific *BRCA2* knockdown mice

Seven days following the administration of 20 mg/kg Dox, heart issues were collected, the left ventricle isolated, and mounted in paraffin and sectioned onto microscope slides and stained with picrosirius red (**Figure 14A**). Cardiac fibrosis was measured via threshold analysis on ImageJ, wherein the % area coverage of collagen-stained Sirius red was calculated against picric-stained cardiac tissue. In both males and females, all mouse groups administered 20 mg/kg Dox displayed significant increase in % area coverage of collagen compared to vehicle-treated WT mice.

Additionally, male BRCA2^{het} and BRCA2^{endo} mice administered 20 mg/kg Dox showed increased fibrosis compared to their vehicle-treated counterparts (**Figure 14B**). In females, only BRCA2^{endo} mice administered 20 mg/kg Dox showed increased fibrosis compared to vehicle-treated littermates (**Figure 14C**).

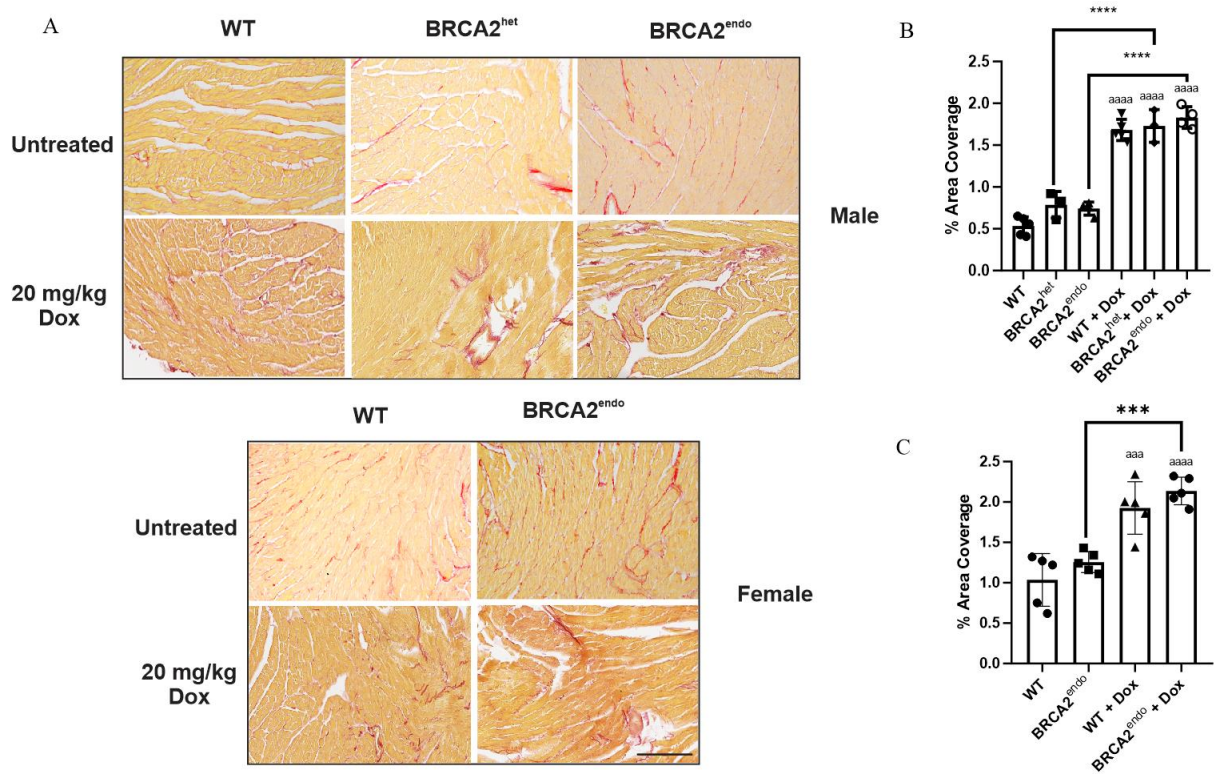

Figure 14. Higher Dox dose significantly increases fibrosis in the hearts of EC-specific *BRCA2* knockdown mice. (A) Heart sections (5 µm) stained for picrosirius red in EC-specific *BRCA2* knockdown mice treated with 20 mg/kg Dox to demonstrate changes in collagen deposition vs. untreated WT. Scale bar = 1 mm. Quantification of (B) male and (C) female cardiac fibrosis in % area coverage of picrosirius red. Data presented as mean +/- SD. aaa, aaaa indicates statistical significance vs. WT, p<0.001, 0.0001 respectively; *, **** indicates statistical significance, p<0.05, p<0.0001, one-way ANOVA, n=3-5 per group, 8-10 weeks old male and female mice.

4.2 Evaluating the loss of *BRCA2* in Dox-induced endotheliotoxicity *in vitro*

4.2.1 Dox treatment up-regulated *BRCA2* expression in HUVECs

After documenting the deleterious effects of Dox in the context of EC-specific loss of *BRCA2*, we turned to *in vitro* cell culture models to uncover the functional mechanisms of Dox exposure directly on endothelial cells. Utilizing HUVECs, we first wanted to establish the dose at which Dox would confer changes in BRCA2 and p53 expression. The dose range (0.5, 1. 2.5, 5 µM) was established based on previous literature (Lorenzo et al., 2002; Maestre et al., 2001). There was an increase in *BRCA2* mRNA expression (**Figure 15A**) and protein level (**Figure 15B**) at 5 µM Dox. Due to the increase of BRCA2, indicating a need to increase in DNA damage repair, we measured pro-apoptotic p53 expression levels. However, no significant changes in p53 levels were observed across the tested doses (**Figure 15C, D**).

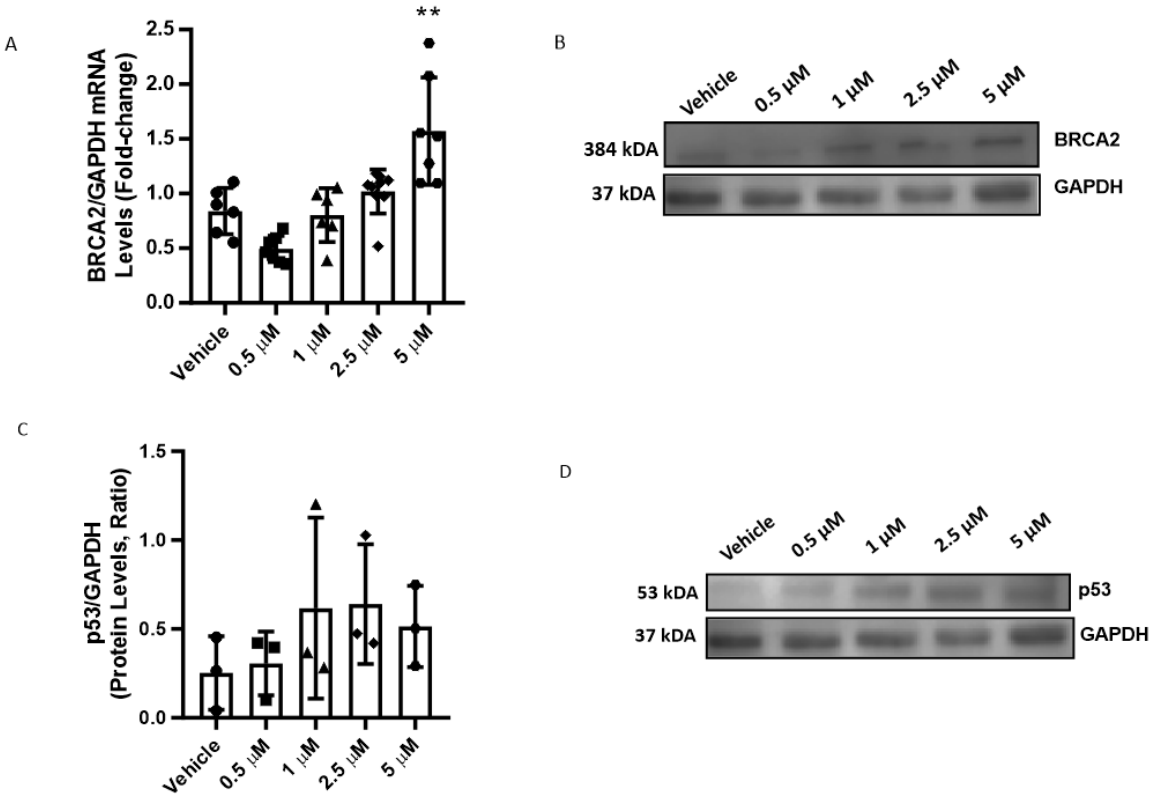

Figure 15. Dox treatment up-regulates *BRCA2* expression in HUVECs. Quantification of BCRA2 (A) mRNA and (B) protein expression; and p53 mRNA (C) and protein (D) expression in HUVECs 18 hours following Dox treatment (Vehicle, 0.5, 1, 2.5 and 5, and 10 µM). *BCRA2* mRNA expression levels were increased in HUVECs treated with 5 µM Dox compared to vehicle treated HUVECs. Data presented as mean +/- SD. ** indicates statistical significance, $p<0.01$ vs. Vehicle control, one-way ANOVA, n=3 performed in triplicate per group.

4.2.2 Dox treatment reduced cell proliferation in *BRCA2*-deficient HUVECs and HCAECs

To assess the effect of *BRCA2* and Dox-treatment on cell proliferation, reverse transfection, a technique that utilizes the addition of gene silencing agents prior to the seeding of cells, was employed to silence *BRCA2 in vitro*. 2.5 µM Dox was then added 48 hours post-transfection for 20 hours and total cell number was counted for HUVECs, and WST-1 absorbance was utilized for HCAECs. In HUVECs silenced for *BRCA2* (si*BRCA2*), a significant increase in cell count was observed compared to scramble (Scr) control, and both Scr control and si*BRCA2* HUVECs showed a decreased cell count compared to vehicle treated controls (**Figure 16A**). In HCAECs, both Dox-treated Scr and *BRCA2*-silenced cells showed a significant decrease in WST-1 absorbance compared to vehicle treated controls, indicating reduced cell proliferation (**Figure 16B**).

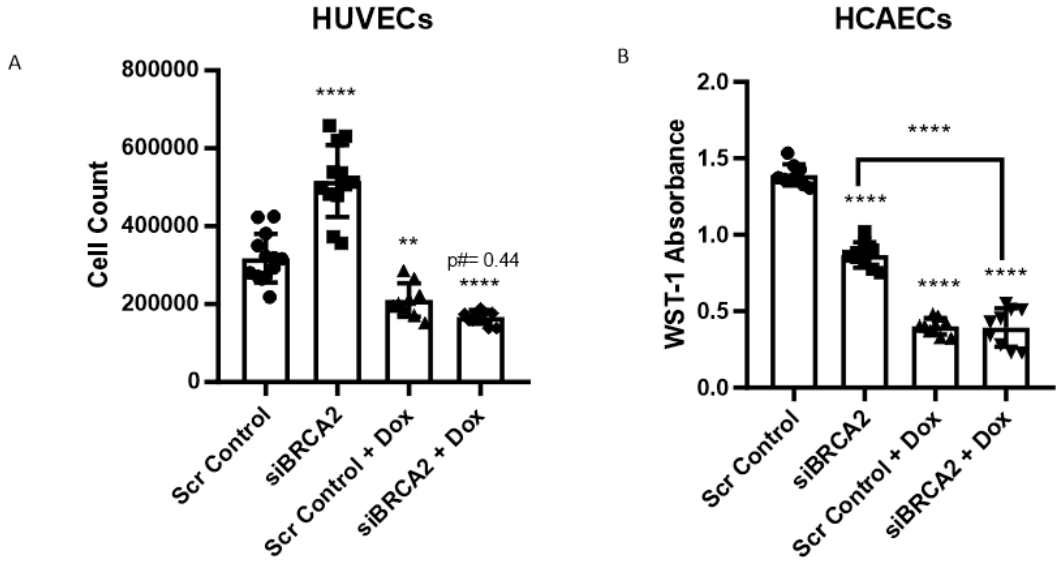

Figure 16. Dox treatment reduced proliferation in both *BRCA2*-silenced and control HUVECs and HCAECs. (A) Cell counts for HUVECs and (B) WST-1 absorbance for HCAECs knocked down for *BRCA2* and treated with 2.5 µM Dox for 20 hours. si*BRCA2* groups in HUVECs and HCAECs both showed changes proliferation compared to Scr Control. Dox reduced proliferation in Scr Control, which was equally reduced in si*BRCA2* + Dox compared to Scr Control. Data presented as mean +/- SD. **, **** indicates statistical significance, p<0.001, 0.0001 vs. Scramble Control (apart from HCAEC si*BRCA2* vs si*BRCA2* + Dox), #p= vs Scr Control + Dox, one-way ANOVA, n=6 per group.

4.2.3 Dox treatment inhibited the migratory capacity of *BRCA2*-deficient HUVECs and HCAECs

The migratory capacity of *BRCA2*-silenced HUVECs and HCAECs was assessed using 2.5 µM Dox treatment. After silencing *BRCA2* for 48 hours, scratch tests were performed and then migration of cells toward the empty area was analyzed at 0, 8, and 20 hours. In HUVECs, migration rate was decreased in *BRCA2*-silenced cells treated with Dox as compared to Scr control (**Figure 17A, B**). However, in HCAECs, migration rate was decreased in both Dox-treated groups compared to control cells (**Figure 17C, D**).

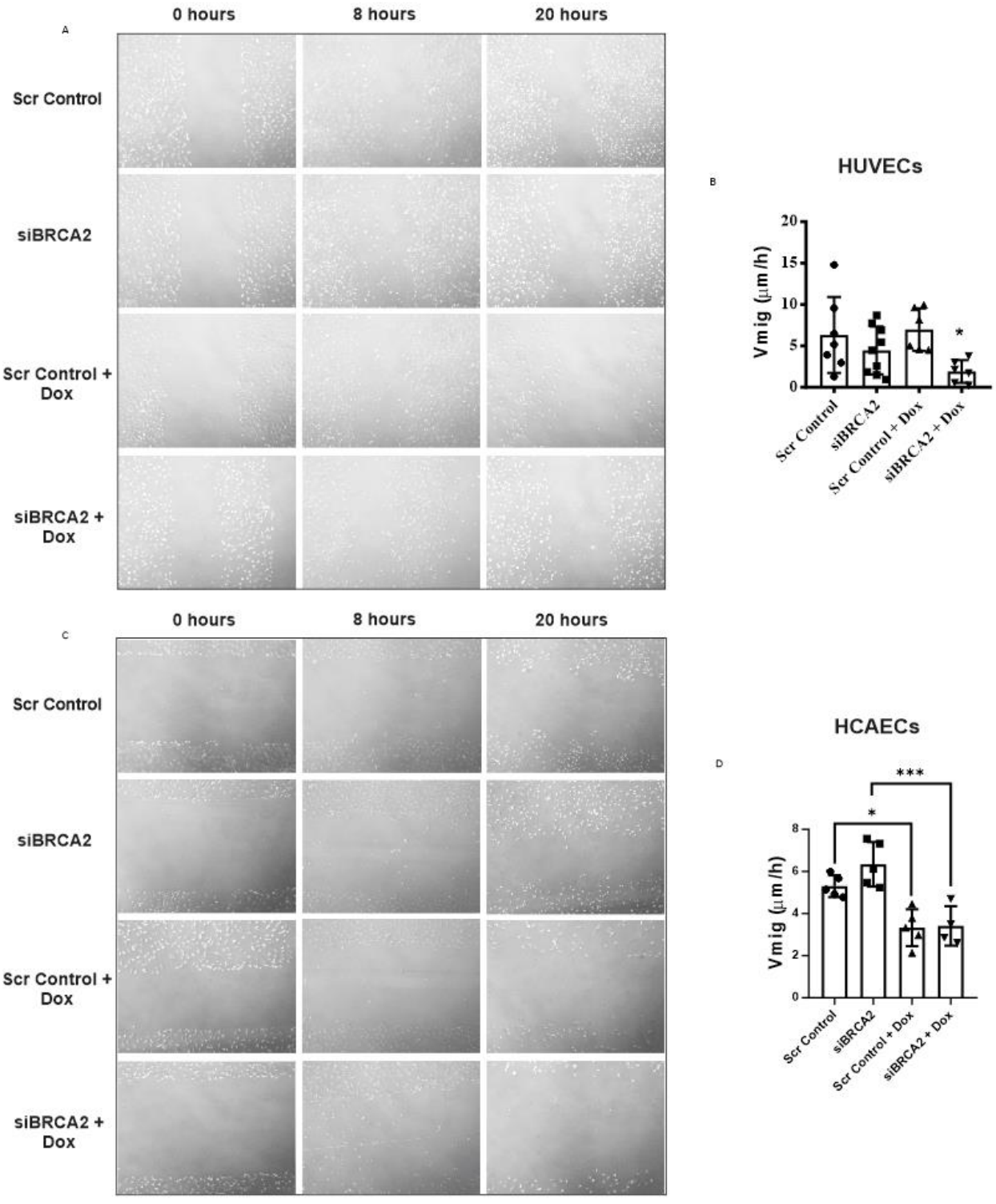

Figure 17. Dox treatment inhibited migratory capacity of *BRCA2*-deficient HUVECs and HCAECs. Representative images of migratory capability of dox-treated (2.5 µM). (A) HUVECs and (C) HCAECs silenced for

BRCA2 for 48 hours; images were taken at 0, 8, and 20 hours. Quantification of migration (µm/hour) for (B) HUVECs and (D) HCAECs. HUVECs showed reduced migration in si*BRCA2* + Dox compared to Scr Control. HCAECs showed reduced migration in Scr Control + Dox compared to Scr Control as well as reduced migration in si*BRCA2* + Dox compared to si*BRCA2*. Data presented as mean +/- SD. *, *** indicates statistical significance, $p<0.05$, 0.001 (*, $p<0.05$ vs. Scr Control in HUVECs), one-way ANOVA, n=3 in triplicates per group**.**

4.2.4 Tube forming capacity was decreased in Dox-treated *BRCA2*-silenced HUVECs

Utilizing knockdown of *BRCA2* in HUVECs, tube forming capacity was assessed after the administration of 2.5 µM Dox. *BRCA2* was silenced for 48 hours and then cells were seeded in a matrix based In Vitro Angiogenesis Assay kit (Millipore). 2.5 µM of Dox was administered and imaging was performed after 4 hours. Dox-treated *BRCA2*-silenced cells showed a significant decrease in tube mesh area compared to Scr control (**Figure 18A, B**).

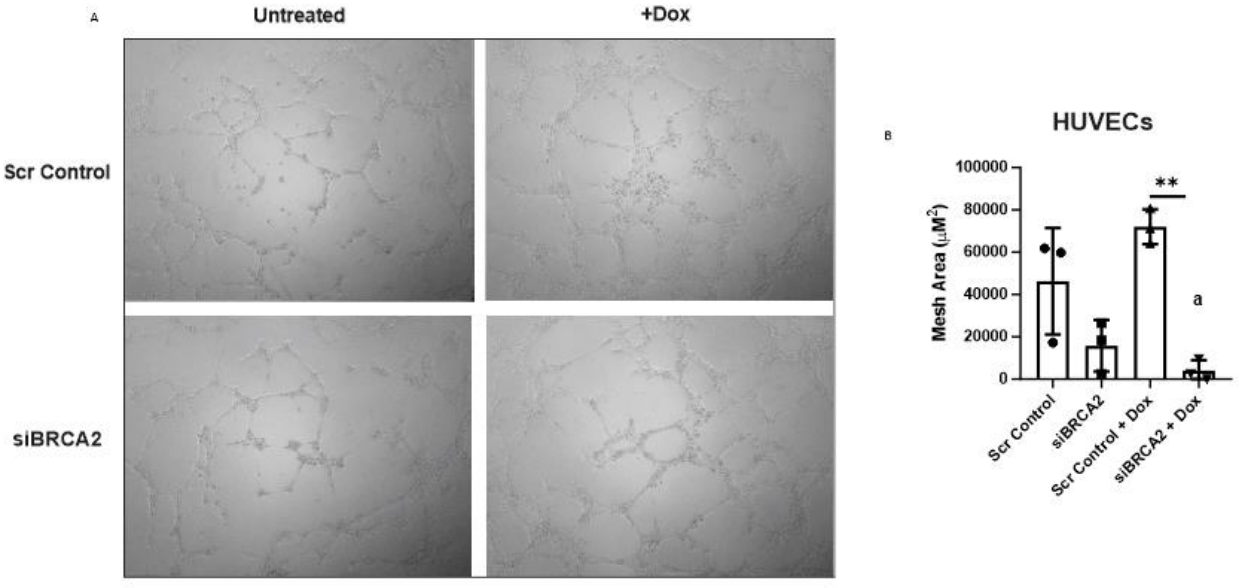

Figure 18. Tube forming capacity is decreased in Dox-treated *BRCA2*-silenced HUVECs. (A) Representative images of tube forming capacity of HUVECs silenced for *BRCA2* for 48 hours and treated with 2.5 µM Dox; images were taken 4 hours later. (B) Quantification of mesh area in μm^2. HUVECs show reduced mesh area formation in

si*BRCA2* + Dox compared to Scr Control + Dox. Data presented as mean +/- SD. a, ** indicates statistical significance, $p<0.05$ vs. Scramble control, $p<0.01$ respectively, one-way ANOVA, n=3 per group.

5 DISCUSSION

The manifestation of cardiac complications in oncology therapeutics is a significant concern to clinicians and patients. Anthracyclines, such as Dox, are a class of chemotherapeutics that are highly used for breast and ovarian cancers. However, due to concerns of anthracycline-induced cardiac dysfunction, Dox use is limited. Furthermore, the pathophysiological factors that predispose individuals to cancer are commonly associated with cardiovascular diseases, such as atherosclerosis (Bosman et al., 2021). Cardiovascular complications following therapeutic intervention are believed to be the result of increased DNA damage induced by anthracycline administration, especially in individuals with *BRCA* mutations (Ahmad et al., 2012; MacDonald et al., 2013; Ruddy et al., 2017). The cytotoxic complications of the loss of *BRCA2* after Dox exposure are the result of overlapping pathways, notably inhibition of eNOS, increased oxidative stress, and increased inflammation in the myocardial endothelium (Wolf & Baynes, 2006). Singh *et al*. demonstrated that Dox-administration to mice with cardiomyocyte-specific *BRCA2* knockdown had greater inflammation, cardiac dysfunction, and p53-dependent apoptosis (K. K. Singh et al., 2012). The role of the endothelium, the innermost cell layer of all blood vessels that act as a barrier against noxious agents, has not been extensively investigated in DIC and no evidence is available concerning the association of *BRCA2* mutation with endothelial function in the context of Dox treatment. Therefore, we employed the *Cre-Lox P* system to create EC-specific *BRCA2* knockdown mice. To study the functional and molecular impact of Dox treatment in our EC-specific *BRCA2* knockdown mice, we started with a lower dose (10 mg/kg) to avoid untoward mortality (K. K. Singh et al., 2012). To document cardiac dysfunction in our mice, LVEF and LVFS were assessed by echocardiography. LVEF represents cardiac output and is an appropriate

measure assessing the risk of coronary artery disease and cardiac health (Motawea et al., 2022). Compromised LVEF can be the result of dilated cardiomyopathy (Japp et al., 2016), myocardial infarction (Motawea et al., 2022), and chronic hypertension (Rosenkranz et al., 2016). LVFS assesses cardiac contractility which is reduced during coronary artery disease (GALDERISI et al., 2007). Impaired contractile function of the heart can also be the result of impaired endothelial function and altered paracrine signalling between endothelial cells and cardiomyocytes (Noireaud & Andriantsitohaina, 2014). The value of assessing LVEF and LVFS is relevant in our BRCA2^{endo} mice as clinical studies often utilize LVEF and LVFS for the characterization of cardiac dysfunction. Seven days post-administration of Dox, both male and female BRCA2^{het} and BRCA2^{endo} mice exhibited significant weight loss, whereas only the BRCA2^{endo} mice showed reduced LVEF and LVFS. Importantly, EC-specific *BRCA2* knockdown mice did not show any differences in cardiac function or weight at baseline compared to WT mice, suggesting the observed weight loss and cardiac dysfunction may arise due to endothelial dysfunction after deletion of endothelial *BRCA2* and Dox treatment.

This is the first study to characterize the effects endothelial *BRCA2* knockdown in the context of Dox treatment. Previous studies from our group investigated DIC using different endothelial-specific knockdowns reported similar findings (A. Z. Luu et al., 2021; V. Z. Luu et al., 2020). Luu *et al.* investigated the role of EC-specific loss of intraflagellar transport protein 88 (**IFT88**) in Dox-induced cardiotoxicity (V. Z. Luu et al., 2020). Interestingly, in EC-specific IFT88 knockdown mice administered Dox, there were no significant differences in cardiac vacuolization, cardiac structural changes, and indices of cardiomyocyte damage compared to WT controls. The same group also investigated the effect of EC-specific loss of autophagy-related protein 7 in Dox-induced cardiotoxicity, reporting increased mortality, cardiac function, and fibrosis. Although

different mechanisms were being investigated in each endothelial cell-specific knockdown model, our findings of compromised cardiac function after Dox treatment in BRCA2^{endo} mice emphasizes the key role of the endothelium in preserving cardiac function.

To address cardiac dysfunction at the molecular level in BRCA2^{endo} mice, we collected heart tissues following the administration of Dox and assessed transcriptional changes of the heart failure markers *BNP*, *aMHC*, *bMHC*, and *FABP3*. These markers have been validated as rodent myocardial injury indicators directly linked to cardiomyocyte degeneration and necrosis (Caforio et al., 2008; Yoshimura et al., 2001; C. Zhu et al., 2011). Injured cardiomyocytes also release enzymes such as creatine kinase into the blood, however, this marker was only successful in characterizing acute cardiomyopathy in rodents whereas *BNP*, *aMHC*, and *bMHC* have all been reported as reliable indicators of chronic cardiomyopathy (Caforio et al., 2008). These markers represent clinical measures of heart failure many years after Dox treatment (Cardinale et al., 2015). In BRCA2^{WT} mice administered Dox, only BNP was upregulated after Dox administration. However, in the absence of Dox, no heart failure markers were elevated between WT or BRCA2^{endo} mice. Furthermore, in mice treated with 10 mg/kg Dox, all heart failure markers were elevated in BRCA2^{endo} mice compared to vehicle treated WT mice. Previous studies assessing Dox-induced cardiomyopathy have reported increased *BNP* (Belen et al., 2022) , *aMHC* and *bMHC* (Chen et al., 2015), as well as FAPB3 (Pan et al., 2022). Our study observed increased expression of these markers during Dox-induced cardiomyopathy, suggesting increased Dox access to cardiomyocytes potentially due to a dysfunctional/leaky endothelium caused by the absence of *BRCA2* function.

To further validate the Dox-induced cardiac dysfunction in our mouse model and characterize whether the mice pathologically exhibited Dox-induced dilated cardiomyopathy as observed in

heart failure patients, we histologically stained the left ventricle of the heart tissues with H&E and picrosirius red. Histopathological hallmarks of dilated cardiomyopathy include increased cardiomyocyte cross-sectional area, hydropic degeneration, interstitial fibrosis, and loss of myofibrils (Mitrut et al., 2018). Previously, it was found that cardiomyocyte-specific *BRCA2* knockdown increased cardiomyocyte area and interstitial fibrosis after Dox treatment (Singh et al., 2012). We sought whether these parameters were also impacted in our EC-specific *BRCA2* knockdown mice. We observed that in both male and female $BRCA2^{het}$ mice, there was a significant increase in cardiomyocyte area following administration of Dox. Dox-administered male and female mice also demonstrated increases in interstitial fibrosis across all groups. To our knowledge, we are the first to demonstrate an increase of cardiomyocyte cross-sectional area following Dox administration through histological measures (Gomes-Santos et al., 2021; Sishi et al., 2013; Sturgeon et al., 2015; Willis et al., 2019). Interestingly, Willis *et al*. report that mice administered 20 mg/kg Dox and euthanized 7 days later showed decreased cardiomyocyte cross-sectional area, indicative of cardiac atrophy. Furthermore, Willis *et al*. reported significantly smaller heart mass after dox-treatment compared to saline-treated mice (Willis et al., 2019). Conversely, our Dox-treated mice had qualitatively larger hearts and increased cross-sectional area, suggesting Dox-induced hypertrophy indicative of dilated cardiomyopathy. In addition, our findings of increased interstitial fibrosis in WT and $BRCA^{endo}$ mice were consistent with similar studies utilizing Dox in murine models (Krishnamurthy et al., 2015; Meléndez et al., 2018; Pei et al., 2014). Overall, our findings were consistent with the complex heterogeneity of heart failure in the context of Dox-induced cardiac dysfunction.

Collectively, our *in vivo* data demonstrate that mice with EC-specific loss of *BRCA2* treated with Dox showed increased cardiac dysfunction evidenced by decreased LVEF and LVFS, increased

heart failure marker expression, and increased cardiomyocyte area and interstitial fibrosis. However, at 10 mg/kg, none of our mice died before being euthanized at 7 days post-Dox administration. Therefore, we increased our dose to 20 mg/kg to investigate changes in mortality in our EC-specific *BRCA2* knockdown mice. Compared to Dox-administered (20 mg/kg) WT mice, Dox-administered BRCA2^{endo} mice exhibited increased mortality. In surviving mice at day 7, we also performed echocardiography for LVEF and LFFS and collected heart tissue for dilated cardiomyopathy assessment via H&E (cardiomyocyte cross-sectional area) and PR (interstitial fibrosis). Due to limited N values at the time of finalization of data for this thesis report, female BRCA2^{het} mice were not assessed across any of the parameters and female echocardiography data was not included. Of the assessed mice, male BRCA2^{endo} mice treated with 20 mg/kg Dox exhibited significant weight loss, and decreased LVEF and LVFS, compared to BRCA2^{endo} mice treated with vehicle. Finally, histopathological data were comparable to that of 10 mg/kg, whereby the only notable differences at 20 mg/kg were increased male cardiomyocyte area in the Dox-administered BRCA2^{endo} mice and the loss of statistical significance for BRCA2^{het} mice treated with Dox.

Having established augmented DIC after EC-specific loss of *BRCA2 in vivo*, we aimed to better understand the role of *BRCA2* in Dox-induced endotheliotoxicity. *BRCA2* transcript levels were increased at 5 µM Dox in *BRCA2*-silenced HUVECs. However, p53 protein levels did not show significant changes compared to vehicle-treated ECs. Nonetheless, these data set the precedent for Dox dose for the remainder of the *in vitro* experiments at 2.5 µM, as we were primarily interested validating changes in *BRCA2* expression *in vivo* after Dox administration, indicating a need for an increase in DNA damage repair.

The remaining experiments were tailored to assess endothelial function by investigating changes in proliferation, migration, and tube formation. Utilizing siRNA mediated knockdown of *BRCA2* in HUVECs and HCAECs, we found decreased proliferation and migration in both Dox-treated *BRCA2*-deficient HUVECs and HCAECs, and reduced tube forming capacity in Dox-treated *BRCA2*-deficient HUVECs. Singh *et al.* previously reported the effect of *BRCA2* knockdown in HUVECs, reporting exacerbated endothelial dysfunction characterized by reduced tube forming capacity in HUVECs treated with oxidized LDL (S. Singh et al., 2020). Although some studies in the literature have investigated the effect of loss of *BRCA2* in HUVECs or HCAECs, numerous studies have investigated the impact of Dox on endothelial function. For instance, Zhang *et al.* reported that HUVECs treated with Dox resulted in reduced migration, but not proliferation (Zhang et al., 2020). We are the first to characterize the loss of *BRCA2* in endothelial cells and investigate the impact of Dox *in vitro*.

Taken together, the novel findings from this project provide the first insight into the role of endothelial *BRCA2* in DIC and forms the foundation for mechanistic studies to follow.

6 CONLCUSIONS, LIMITATIONS, FUTURE DIRECTIONS

6.1 Conclusions

The findings from this thesis elucidate the important role of *BRCA2* in maintaining the integrity of endothelium, particularly in the presence of stressors such as Dox. EC-specific *BRCA2* knockdown mice exhibit increased mortality, weight loss, decreased LVEF and LVFS, increased expression of heart failure markers and dilated cardiomyopathy evidenced by increased interstitial fibrosis and cardiomyocyte area. In addition, Dox-treatment in *BRCA2*-silenced ECs exhibited endothelial dysfunction evidenced by decreased cellular proliferation, migration, and tube-forming capacity *in vitro*. Overall, our data suggest that BRCA2 depletion severely compromises endothelial function after Dox-exposure, leading to increased permeability and subsequent increase of Dox infiltration to the heart tissue, and exacerbated DIC. Our data also suggests that genotoxic therapeutics may exacerbate CVD in patients with *BRCA2* mutations and/or haploinsufficiency (**Figure 19**).

6.2 Limitations

There are several limitations to our study. Primarily, statistically insignificant relationships were apparent, but some assessments did not reach significance due to a limited number of animal/experiments (e.g., the increase in p53 in HUVECs treated with Dox in a dose-dependent manner). Increasing the number of mice in each group, and importantly, representing female EC-specific $BRCA2^{het}$ mice administered Dox, is important for conclusive relationships to be stated. Although the mechanistic implications of Dox-induced cardiotoxicity or endothelial dysfunction were thoroughly investigated, current experiments are underway with protein and RNA from tissue and cell digests to investigate markers of apoptosis, DNA damage, inflammation, and oxidative

stress. Immunofluorescence experiments are also underway to spatially localize the expression of markers involved for the abovementioned parameters. These limitations will be addressed prior to knowledge transfer of our findings to the scientific community.

6.3 Future Directions

In the future, studies can be aimed at investigating a multi-dose application of Dox in our mouse model. In the clinic, patients are rarely administered a single cycle of Dox and many studies utilizing Dox in knockdown murine models administer Dox over a more chronic time period with multiple injections. Letting our mice recover and age between rounds of lower-dose Dox administration would also be more clinically relevant as there are many patients who develop heart failure many years following multiple Dox treatments. It would also be valuable to perform RNAseq on isolated mouse cardiac tissue (cardiomyocytes, fibroblasts and endothelial cells) from our Dox-treated BRCA2^{endo} and WT mice to better understand the role of endothelial-cardiomyocyte interaction in DIC. Altogether, these studies may unveil important mechanistic interactions of endothelial cells and cardiomyocytes under multiple experimental models and Dox-dosing conditions, increasing the validity of our findings and cementing BRCA2 as a key protective regulator of the endothelium under stress.

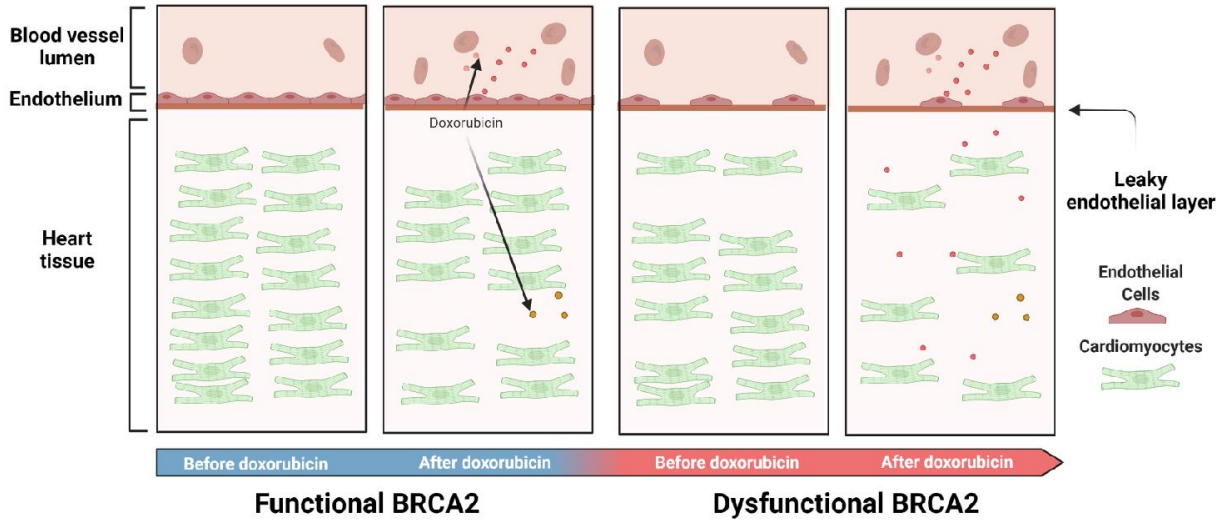

Figure 19. Summary schematic. The endothelium acts as the first layer of contact against agents within the systemic circulation; if the endothelium is compromised, harmful agents can reach the functional units of the heart, the cardiomyocytes, and create a cardiotoxic environment. In the case of doxorubicin, an amphoteric chemotherapeutic agent, the endothelium prevents a significant amount of doxorubicin from reaching the cardiomyocytes within the heart; however, individuals who have dysfunctional BRCA2 often end up having a leaky endothelium (which is exacerbated by doxorubicin). These individuals may be at increased risk of developing heart failure following the administration of doxorubicin. It is imperative that these patients are not administered genotoxic drugs such as doxorubicin to prevent unwanted therapeutic outcomes.

REFERENCES

Ahmad, S. S., Duke, S., Jena, R., Williams, M. V., & Burnet, N. G. (2012). Advances in radiotherapy. *BMJ*, *345*(dec04 1), e7765–e7765. https://doi.org/10.1136/bmj.e7765

Alacacioglu, A., Varol, U., Kucukzeybek, Y., Somali, I., Altun, Z., Aktas, S., & Tarhan, M. O. (2018). BRCA genes: BRCA 1 and BRCA 2. *JBUON*, *23*(4), 862–866.

Amin, F. M., Sharawy, M. H., Amin, M. N., El-Sherbiny, M., Said, E., Salem, H. A., & Ibrahim, T. M. (2023). Nifuroxazide mitigates doxorubicin-induced cardiovascular injury: Insight into oxidative/NLRP3/GSDMD-mediated pyroptotic signaling modulation. *Life Sciences*, *314*, 121311. https://doi.org/10.1016/j.lfs.2022.121311

Ballinger, S. W., Patterson, C., Knight-Lozano, C. A., Burow, D. L., Conklin, C. A., Hu, Z., Reuf, J., Horaist, C., Lebovitz, R., Hunter, G. C., McIntyre, K., & Runge, M. S. (2002). Mitochondrial Integrity and Function in Atherogenesis. *Circulation*, *106*(5), 544–549. https://doi.org/10.1161/01.CIR.0000023921.93743.89

Baretta, Z., Mocellin, S., Goldin, E., Olopade, O. I., & Huo, D. (2016). Effect of BRCA germline mutations on breast cancer prognosis: A systematic review and meta-analysis. *Medicine (United States)*, *95*(40). https://doi.org/10.1097/MD.0000000000004975

Belen, E., Canbolat, I. P., Yigittürk, G., Cetinarslan, Ö., Akdeniz, C. S., Karaca, M., Sönmez, M., & Erbas, O. (2022). Cardio-protective effect of dapagliflozin against doxorubicin induced cardiomyopathy in rats. *European Review for Medical and Pharmacological Sciences*, *26*(12), 4403–4408. https://doi.org/10.26355/eurrev_202206_29079

Bordeleau, L., Lipscombe, L., Lubinski, J., Ghadirian, P., Foulkes, W. D., Neuhausen, S., Ainsworth, P., Pollak, M., Sun, P., & Narod, S. A. (2011). Diabetes and breast cancer among women with BRCA1 and BRCA2 mutations. *Cancer*, *117*(9), 1812–1818. https://doi.org/10.1002/cncr.25595

Bosman, M., Favere, K., Neutel, C. H. G., Jacobs, G., De Meyer, G. R. Y., Martinet, W., Van Craenenbroeck, E. M., & Guns, P.-J. D. F. (2021). Doxorubicin induces arterial stiffness: A comprehensive in vivo and ex vivo evaluation of vascular toxicity in mice. *Toxicology Letters*, *346*, 23–33. https://doi.org/10.1016/j.toxlet.2021.04.015

Boulton, S. J. (2006). Cellular functions of the BRCA tumour-suppressor proteins. *Biochemical Society Transactions*, *34*(5), 633–645. https://doi.org/10.1042/BST0340633

Busse, R., & Fleming, I. (n.d.). Vascular Endothelium and Blood Flow. In *The Vascular Endothelium II* (pp. 43–78). Springer Berlin Heidelberg. https://doi.org/10.1007/3-540-36028-X_2

Caforio, A. L. P., Vinci, A., & Iliceto, S. (2008). Anti-heart autoantibodies in familial dilated cardiomyopathy. *Autoimmunity*, *41*(6), 462–469. https://doi.org/10.1080/08916930802031546

Cain, H., Macpherson, I. R., Beresford, M., Pinder, S. E., Pong, J., & Dixon, J. M. (2017). Neoadjuvant Therapy in Early Breast Cancer: Treatment Considerations and Common Debates in Practice. *Clinical Oncology*, *29*(10), 642–652. https://doi.org/10.1016/j.clon.2017.06.003

Cardinale, D., Colombo, A., Bacchiani, G., Tedeschi, I., Meroni, C. A., Veglia, F., Civelli, M., Lamantia, G., Colombo, N., Curigliano, G., Fiorentini, C., & Cipolla, C. M. (2015). Early Detection of Anthracycline Cardiotoxicity and Improvement With Heart Failure Therapy. *Circulation*, *131*(22), 1981–1988. https://doi.org/10.1161/CIRCULATIONAHA.114.013777

Chen, Y.-L., Chung, S.-Y., Chai, H.-T., Chen, C.-H., Liu, C.-F., Chen, Y.-L., Huang, T.-H., Zhen, Y.-Y., Sung, P.-H., Sun, C.-K., Chua, S., Lu, H.-I., Lee, F.-Y., Sheu, J.-J., & Yip, H.-K. (2015). Early Administration of Carvedilol Protected against Doxorubicin-Induced Cardiomyopathy. *Journal of Pharmacology and Experimental Therapeutics*, *355*(3), 516–527. https://doi.org/10.1124/jpet.115.225375

Demissei, B. G., Lv, W., Wilcox, N. S., Sheline, K., Smith, A. M., Sturgeon, K. M., McDermott-Roe, C., Musunuru, K., Lefebvre, B., Domchek, S. M., Shah, P., & Ky, B. (2022). BRCA1/2 Mutations and Cardiovascular Function in Breast Cancer Survivors. *Frontiers in Cardiovascular Medicine*, *9*. https://doi.org/10.3389/fcvm.2022.833171

Dyer, L. A., & Patterson, C. (2010). Development of the endothelium: an emphasis on heterogeneity. *Seminars in Thrombosis and Hemostasis*, *36*(3), 227–235. https://doi.org/10.1055/s-0030-1253446

Florey. (1966). The endothelial cell. *British Medical Journal*, *2*(5512), 487–490. https://doi.org/10.1136/bmj.2.5512.487

Foulkes, W. D. (2008). Inherited Susceptibility to Common Cancers. *New England Journal of Medicine*, *359*(20), 2143–2153. https://doi.org/10.1056/NEJMra0802968

GALDERISI, M., DESIMONE, G., CICALA, S., PARISI, M., DERRICO, A., INNELLI, P., DEDIVITIIS, M., MONDILLO, S., & DEDIVITIIS, O. (2007). Coronary Flow Reserve in Hypertensive Patients With Hypercholesterolemia and Without Coronary Heart Disease. *American Journal of Hypertension*, *20*(2), 177–183. https://doi.org/10.1016/j.amjhyper.2006.06.017

Gast, K. C., Viscuse, P. V, Nowsheen, S., Haddad, T. C., Mutter, R. W., Hendrickson, A. E. W., Couch, F. J., & Ruddy, K. J. (2018). Cardiovascular Concerns in BRCA1 and BRCA2 Mutation Carriers. *Current Treatment Options in Cardiovascular Medicine*, *20*(2). https://doi.org/10.1007/s11936-018-0609-z

Gomes-Santos, I. L., Jordão, C. P., Passos, C. S., Brum, P. C., Oliveira, E. M., Chammas, R., Camargo, A. A., & Negrão, C. E. (2021). Exercise Training Preserves Myocardial Strain and Improves Exercise Tolerance in Doxorubicin-Induced Cardiotoxicity. *Frontiers in Cardiovascular Medicine*, *8*. https://doi.org/10.3389/fcvm.2021.605993

Gottlieb, T. M., & Oren, M. (1998). p53 and apoptosis. *Seminars in Cancer Biology*, *8*(5), 359–368. https://doi.org/10.1006/scbi.1998.0098

He, H., Wang, L., Qiao, Y., Zhou, Q., Li, H., Chen, S., Yin, D., Huang, Q., & He, M. (2020). Doxorubicin Induces Endotheliotoxicity and Mitochondrial Dysfunction via ROS/eNOS/NO Pathway. *Frontiers in Pharmacology*, *10*. https://doi.org/10.3389/fphar.2019.01531

Heijink, A. M., Talens, F., Jae, L. T., van Gijn, S. E., Fehrmann, R. S. N., Brummelkamp, T. R., & van Vugt, M. A. T. M. (2019). BRCA2 deficiency instigates cGAS-mediated inflammatory signaling and confers sensitivity to tumor necrosis factor-alpha-mediated cytotoxicity. *Nature Communications*, *10*(1), 100. https://doi.org/10.1038/s41467-018-07927-y

Hughes, D. J., Ginolhac, S. M., Coupier, I., Corbex, M., Bressac-de-Paillerets, B., Chompret, A., Bignon, Y.-J., Uhrhammer, N., Lasset, C., Giraud, S., Hardouin, A., Berthet, P., Peyrat, J.-P., Fournier, J., Nogues, C., Lidereau, R., Muller, D., Fricker, J.-P., Longy, M., … Sinilnikova, O. M. (2005). Common BRCA2 variants and modification of breast and ovarian cancer risk in BRCA1 mutation carriers. *Cancer Epidemiology, Biomarkers & Prevention : A Publication of the American Association for Cancer Research, Cosponsored by the American Society of Preventive Oncology*, *14*(1), 265–267.

Incalza, M. A., D'Oria, R., Natalicchio, A., Perrini, S., Laviola, L., & Giorgino, F. (2018). Oxidative stress and reactive oxygen species in endothelial dysfunction associated with cardiovascular and metabolic diseases. *Vascular Pharmacology*, *100*, 1–19. https://doi.org/10.1016/j.vph.2017.05.005

Jambusaria, A., Hong, Z., Zhang, L., Srivastava, S., Jana, A., Toth, P. T., Dai, Y., Malik, A. B., & Rehman, J. (2020). Endothelial heterogeneity across distinct vascular beds during homeostasis and inflammation. *ELife*, *9*. https://doi.org/10.7554/eLife.51413

Japp, A. G., Gulati, A., Cook, S. A., Cowie, M. R., & Prasad, S. K. (2016). The Diagnosis and Evaluation of Dilated Cardiomyopathy. *Journal of the American College of Cardiology*, *67*(25), 2996–3010. https://doi.org/10.1016/j.jacc.2016.03.590

Jerusalem, G., Lancellotti, P., & Kim, S.-B. (2019). HER2+ breast cancer treatment and cardiotoxicity: monitoring and management. *Breast Cancer Research and Treatment*, *177*(2), 237–250. https://doi.org/10.1007/s10549-019-05303-y

Johnson, A. F., Nguyen, H. T., & Veitia, R. A. (2019). Causes and effects of haploinsufficiency. *Biological Reviews*, *94*(5), 1774–1785. https://doi.org/10.1111/brv.12527

Jonkman, J. E. N., Cathcart, J. A., Xu, F., Bartolini, M. E., Amon, J. E., Stevens, K. M., & Colarusso, P. (2014). An introduction to the wound healing assay using live-cell microscopy. *Cell Adhesion & Migration*, *8*(5), 440–451. https://doi.org/10.4161/cam.36224

Kawale, A. S., & Sung, P. (2020). Mechanism and significance of chromosome damage repair by homologous recombination. *Essays in Biochemistry*, *64*(5), 779–790. https://doi.org/10.1042/EBC20190093

Khan, B. V, Parthasarathy, S. S., Alexander, R. W., & Medford, R. M. (1995). Modified low density lipoprotein and its constituents augment cytokine-activated vascular cell adhesion molecule-1 gene expression in human vascular endothelial cells. *Journal of Clinical Investigation*, *95*(3), 1262–1270. https://doi.org/10.1172/JCI117776

Kim, Y. A., Cho, H., Lee, N., Jung, S. Y., Sim, S. H., Park, I. H., Lee, S., Lee, E. S., & Kim, H. J. (2018). Doxorubicin-induced heart failure in cancer patients: A cohort study based on the Korean National Health Insurance Database. *Cancer Medicine*, *7*(12), 6084–6092. https://doi.org/10.1002/cam4.1886

Knapp, M., Tu, X., & Wu, R. (2019). Vascular endothelial dysfunction, a major mediator in diabetic cardiomyopathy. *Acta Pharmacologica Sinica*, *40*(1), 1–8. https://doi.org/10.1038/s41401-018-0042-6

Koutroumpakis, E., Palaskas, N. L., Lin, S. H., Abe, J., Liao, Z., Banchs, J., Deswal, A., & Yusuf, S. W. (2020). Modern Radiotherapy and Risk of Cardiotoxicity. *Chemotherapy*, *65*(3–4), 65–76. https://doi.org/10.1159/000510573

Krishnamurthy, B., Rani, N., Bharti, S., Golechha, M., Bhatia, J., Nag, T. C., Ray, R., Arava, S., & Arya, D. S. (2015). Febuxostat ameliorates doxorubicin-induced cardiotoxicity in rats. *Chemico-Biological Interactions*, *237*, 96–103. https://doi.org/10.1016/j.cbi.2015.05.013

Krupina, K., Goginashvili, A., & Cleveland, D. W. (2021). Causes and consequences of micronuclei. *Current Opinion in Cell Biology*, *70*, 91–99. https://doi.org/10.1016/j.ceb.2021.01.004

Kuchenbaecker, K. B., Hopper, J. L., Barnes, D. R., Phillips, K.-A., Mooij, T. M., Roos-Blom, M.-J., Jervis, S., van Leeuwen, F. E., Milne, R. L., Andrieu, N., Goldgar, D. E., Terry, M. B., Rookus, M. A., Easton, D. F., Antoniou, A. C., McGuffog, L., Evans, D. G., Barrowdale, D., Frost, D., … Olsson, H. (2017). Risks of Breast, Ovarian, and Contralateral Breast Cancer for *BRCA1* and *BRCA2* Mutation Carriers. *JAMA*, *317*(23), 2402. https://doi.org/10.1001/jama.2017.7112

Liao, Y.-C., Lin, H.-F., Guo, Y.-C., Chen, C.-H., Huang, Z.-Z., Juo, S.-H. H., & Lin, R.-T. (2013). Lack of association between a functional variant of the BRCA-1 related associated protein (BRAP) gene and ischemic stroke. *BMC Medical Genetics*, *14*(1), 17. https://doi.org/10.1186/1471-2350-14-17

Lin, F., Yang, Y., Wei, S., Huang, X., Peng, Z., Ke, X., Zeng, Z., & Song, Y. (2020). Hydrogen Sulfide Protects Against High Glucose-Induced Human Umbilical Vein Endothelial Cell Injury Through Activating PI3K/Akt/eNOS Pathway. *Drug Design, Development and Therapy*, *Volume 14*, 621–633. https://doi.org/10.2147/DDDT.S242521

Lord, R. S. A., & Bobryshev, Y. V. (2002). Hallmarks of Atherosclerotic Lesion Development with Special Reference to Immune Inflammatory Mechanisms. *Cardiovascular Surgery*, *10*(4), 405–414. https://doi.org/10.1177/096721090201000422

Lorenzo, E., Ruiz-Ruiz, C., Quesada, A. J., Hernández, G., Rodríguez, A., López-Rivas, A., & Redondo, J. M. (2002). Doxorubicin Induces Apoptosis and CD95 Gene Expression in Human Primary Endothelial Cells through a p53-dependent Mechanism. *Journal of Biological Chemistry*, *277*(13), 10883–10892. https://doi.org/10.1074/jbc.M107442200

Luu, A. Z., Chowdhury, B., Al-Omran, M., Teoh, H., Hess, D. A., & Verma, S. (2018). Role of Endothelium in Doxorubicin-Induced Cardiomyopathy. *JACC: Basic to Translational Science*, *3*(6), 861–870. https://doi.org/10.1016/j.jacbts.2018.06.005

Luu, A. Z., Luu, V. Z., Chowdhury, B., Kosmopoulos, A., Pan, Y., Al-Omran, M., Quan, A., Teoh, H., Hess, D. A., & Verma, S. (2021). Loss of endothelial cell-specific autophagy-related protein 7 exacerbates doxorubicin-induced cardiotoxicity. *Biochemistry and Biophysics Reports*, *25*, 100926. https://doi.org/10.1016/j.bbrep.2021.100926

Luu, V. Z., Luu, A. Z., Chowdhury, B., Elbardisy, O., Pan, Y., Al-Omran, M., Quan, A., Teoh, H., Hess, D. A., & Verma, S. (2020). Disruption of endothelial cell intraflagellar transport protein 88 exacerbates doxorubicin-induced cardiotoxicity. *Life Sciences*, *260*, 118216. https://doi.org/10.1016/j.lfs.2020.118216

Ma, J., Cai, H., Wu, T., Sobhian, B., Huo, Y., Alcivar, A., Mehta, M., Cheung, K. L., Ganesan, S., Kong, A.-N. T., Zhang, D. D., & Xia, B. (2012). PALB2 interacts with KEAP1 to promote NRF2 nuclear accumulation and function. *Molecular and Cellular Biology*, *32*(8), 1506–1517. https://doi.org/10.1128/MCB.06271-11

MacDonald, S. M., Patel, S. A., Hickey, S., Specht, M., Isakoff, S. J., Gadd, M., Smith, B. L., Yeap, B. Y., Adams, J., DeLaney, T. F., Kooy, H., Lu, H.-M., & Taghian, A. G. (2013). Proton Therapy for Breast Cancer After Mastectomy: Early Outcomes of a Prospective Clinical Trial. *International Journal of Radiation Oncology*Biology*Physics*, *86*(3), 484–490. https://doi.org/10.1016/j.ijrobp.2013.01.038

Maestre, N., Tritton, T. R., Laurent, G., & Jaffrézou, J. P. (2001). Cell surface-directed interaction of anthracyclines leads to cytotoxicity and nuclear factor kappaB activation but not apoptosis signaling. *Cancer Research*, *61*(6), 2558–2561.

Majno, G., & Palade, G. E. (1961). STUDIES ON INFLAMMATION. *The Journal of Biophysical and Biochemical Cytology*, *11*(3), 571–605. https://doi.org/10.1083/jcb.11.3.571

Marmorstein, L. Y., Kinev, A. V, Chan, G. K. T., Bochar, D. A., Beniya, H., Epstein, J. A., Yen, T. J., & Shiekhattar, R. (2001). A Human BRCA2 Complex Containing a Structural DNA Binding Component Influences Cell Cycle Progression. *Cell*, *104*(2), 247–257. https://doi.org/10.1016/S0092-8674(01)00209-4

Marrocco, I., Altieri, F., & Peluso, I. (2017). Measurement and Clinical Significance of Biomarkers of Oxidative Stress in Humans. *Oxidative Medicine and Cellular Longevity*, *2017*, 1–32. https://doi.org/10.1155/2017/6501046

Meléndez, G. C., Jordan, J. H., D'Agostino, R. B., Lesnefsky, E. J., & Hundley, W. G. (2018). Accelerated Left Ventricular Interstitial Collagen Deposition After Receiving Doxorubicin in Hypertension. *Journal of the American College of Cardiology*, *72*(13), 1555–1557. https://doi.org/10.1016/j.jacc.2018.07.028

Mitrut, R., Stepan, A. E., & Pirici, D. (2018). Histopathological Aspects of the Myocardium in Dilated Cardiomyopathy. *Current Health Sciences Journal*, *44*(3), 243–249. https://doi.org/10.12865/CHSJ.44.03.07

Motawea, K. R., Gaber, H., Singh, R. B., Swed, S., Elshenawy, S., Talat, N. E., Elgabrty, N., Shoib, S., Wahsh, E. A., Chébl, P., Reyad, S. M., Rozan, S. S., & Aiash, H. (2022). Effect of early metoprolol before PCI in ST-segment elevation myocardial infarction on infarct size and left ventricular ejection fraction. A systematic review and meta-analysis of clinical trials. *Clinical Cardiology*, *45*(10), 1011–1028. https://doi.org/10.1002/clc.23894

Muhammad, W., Khan, M. M., Zafar, S., Alqutub, M. N., AlMubarak, A. M., Mokeem, S., Khan, Z. A., Usman, M. K., Ahmed, N., Aldahiyan, N., Vohra, F., & Abduljabbar, T. (2021). Assessment of Unstimulated Whole Salivary Tumor Necrosis Factor Alpha (TNF-α) and Cellular Micronuclei Levels

in Snuff (Naswar) Users and Non-Users for Early Diagnosis of Oral Squamous Cell Carcinoma. *International Journal of Environmental Research and Public Health*, *18*(14), 7230. https://doi.org/10.3390/ijerph18147230

Nagini, S. (2017). Breast Cancer: Current Molecular Therapeutic Targets and New Players. *Anti-Cancer Agents in Medicinal Chemistry*, *17*(2), 152–163. https://doi.org/10.2174/1871520616666160502122724

Nicolai, S., Rossi, A., Di Daniele, N., Melino, G., Annicchiarico-Petruzzelli, M., & Raschellà, G. (2015). DNA repair and aging: the impact of the p53 family. *Aging*, *7*(12), 1050–1065. https://doi.org/10.18632/aging.100858

Nicolaides, A. N. (2005). Chronic Venous Disease and the Leukocyte-Endothelium Interaction: From Symptoms to Ulceration. *Angiology*, *56*(6_suppl), S11–S19. https://doi.org/10.1177/00033197050560i103

Nicolazzi, M. A., Carnicelli, A., Fuorlo, M., Scaldaferri, A., Masetti, R., Landolfi, R., & Favuzzi, A. M. R. (2018). Anthracycline and trastuzumab-induced cardiotoxicity in breast cancer. *European Review for Medical and Pharmacological Sciences*, *22*(7), 2175–2185. https://doi.org/10.26355/eurrev_201804_14752

Nikfarjam, S., & Singh, K. K. (2023). DNA damage response signaling: A common link between cancer and cardiovascular diseases. *Cancer Medicine*, *12*(4), 4380–4404. https://doi.org/10.1002/cam4.5274

Noireaud, J., & Andriantsitohaina, R. (2014). Recent Insights in the Paracrine Modulation of Cardiomyocyte Contractility by Cardiac Endothelial Cells. *BioMed Research International*, *2014*, 1–10. https://doi.org/10.1155/2014/923805

Pan, D.-S., Li, B., & Wang, S.-L. (2022). Evaluation of biomarkers for doxorubicin-induced cardiac injury in rats. *Experimental and Therapeutic Medicine*, *24*(6), 712. https://doi.org/10.3892/etm.2022.11648

Pearson, E. J., Nair, A., Daoud, Y., & Blum, J. L. (2017). The incidence of cardiomyopathy in BRCA1 and BRCA2 mutation carriers after anthracycline-based adjuvant chemotherapy. *Breast Cancer Research and Treatment*, *162*(1), 59–67. https://doi.org/10.1007/s10549-016-4101-8

Pei, X. M., Yung, B. Y., Yip, S. P., Ying, M., Benzie, I. F., & Siu, P. M. (2014). Desacyl ghrelin prevents doxorubicin-induced myocardial fibrosis and apoptosis via the GHSR-independent pathway. *American Journal of Physiology. Endocrinology and Metabolism*, *306*(3), E311-23. https://doi.org/10.1152/ajpendo.00123.2013

Rawat, P. S., Jaiswal, A., Khurana, A., Bhatti, J. S., & Navik, U. (2021). Doxorubicin-induced cardiotoxicity: An update on the molecular mechanism and novel therapeutic strategies for effective management. *Biomedicine & Pharmacotherapy*, *139*, 111708. https://doi.org/10.1016/j.biopha.2021.111708

Rebbeck, T. R., Mitra, N., Wan, F., Sinilnikova, O. M., Healey, S., McGuffog, L., Mazoyer, S., Chenevix-Trench, G., Easton, D. F., Antoniou, A. C., Nathanson, K. L., Laitman, Y., Kushnir, A., Paluch-Shimon, S., Berger, R., Zidan, J., Friedman, E., Ehrencrona, H., Stenmark-Askmalm, M., … Andrulis, I. (2015).

Association of Type and Location of *BRCA1* and *BRCA2* Mutations With Risk of Breast and Ovarian Cancer. *JAMA*, *313*(13), 1347. https://doi.org/10.1001/jama.2014.5985

Rosenkranz, S., Gibbs, J. S. R., Wachter, R., De Marco, T., Vonk-Noordegraaf, A., & Vachiéry, J.-L. (2016). Left ventricular heart failure and pulmonary hypertension. *European Heart Journal*, *37*(12), 942–954. https://doi.org/10.1093/eurheartj/ehv512

Roy, R., Chun, J., & Powell, S. N. (2012). BRCA1 and BRCA2: Different roles in a common pathway of genome protection. In *Nature Reviews Cancer* (Vol. 12, Issue 1, pp. 68–78). https://doi.org/10.1038/nrc3181

Ruddy, K. J., Van Houten, H. K., Sangaralingham, L. R., Freedman, R. A., Thompson, C. A., Hashmi, S. K., Jemal, A., Haddad, T. C., Mougalian, S., Herrin, J., Gross, C., & Shah, N. (2017). Impact of treatment regimen on acute care use during and after adjuvant chemotherapy for early-stage breast cancer. *Breast Cancer Research and Treatment*, *164*(3), 515–525. https://doi.org/10.1007/s10549-017-4280-y

Salnikova, D., Orekhova, V., Grechko, A., Starodubova, A., Bezsonov, E., Popkova, T., & Orekhov, A. (2021). Mitochondrial Dysfunction in Vascular Wall Cells and Its Role in Atherosclerosis. *International Journal of Molecular Sciences*, *22*(16), 8990. https://doi.org/10.3390/ijms22168990

Sarhangi, N., Hajjari, S., Heydari, S. F., Ganjizadeh, M., Rouhollah, F., & Hasanzad, M. (2022). Breast cancer in the era of precision medicine. *Molecular Biology Reports*, *49*(10), 10023–10037. https://doi.org/10.1007/s11033-022-07571-2

Sener, S. F. (1996). Breast cancer in older women: Screening and selection of locoregional therapy. *Seminars in Surgical Oncology*, *12*(5), 328–331. https://doi.org/10.1002/(SICI)1098-2388(199609/10)12:5<328::AID-SSU7>3.0.CO;2-F

Shah, A. N., & Gradishar, W. J. (2018). Adjuvant Anthracyclines in Breast Cancer: What Is Their Role? *The Oncologist*, *23*(10), 1153–1161. https://doi.org/10.1634/theoncologist.2017-0672

Shukla, P. C., Singh, K. K., Quan, A., Al-Omran, M., Teoh, H., Lovren, F., Cao, L., Rovira, I. I., Pan, Y., Brezden-Masley, C., Yanagawa, B., Gupta, A., Deng, C. X., Coles, J. G., Leong-Poi, H., Stanford, W. L., Parker, T. G., Schneider, M. D., Finkel, T., & Verma, S. (2011). BRCA1 is an essential regulator of heart function and survival following myocardial infarction. *Nature Communications*, *2*(1). https://doi.org/10.1038/ncomms1601

Singh, K. K., Shukla, P. C., Quan, A., Desjardins, J. F., Lovren, F., Pan, Y., Garg, V., Gosal, S., Garg, A., Szmitko, P. E., Schneider, M. D., Parker, T. G., Stanford, W. L., Leong-Poi, H., Teoh, H., Al-Omran, M., & Verma, S. (2012). BRCA2 protein deficiency exaggerates doxorubicin-induced cardiomyocyte apoptosis and cardiac failure. *Journal of Biological Chemistry*, *287*(9), 6604–6614. https://doi.org/10.1074/jbc.M111.292664

Singh, S., Nguyen, H., Michels, D., Bazinet, H., Matkar, P. N., Liu, Z., Esene, L., Adam, M., Bugyei-Twum, A., Mebrahtu, E., Joseph, J., Ehsan, M., Chen, H. H., Qadura, M., & Singh, K. K. (2020). BReast CAncer susceptibility gene 2 deficiency exacerbates oxidized LDL-induced DNA damage and endothelial apoptosis. *Physiological Reports*, *8*(13). https://doi.org/10.14814/phy2.14481

Sishi, B. J. N., Loos, B., van Rooyen, J., & Engelbrecht, A.-M. (2013). Autophagy upregulation promotes survival and attenuates doxorubicin-induced cardiotoxicity. *Biochemical Pharmacology*, *85*(1), 124–134. https://doi.org/10.1016/j.bcp.2012.10.005

Sturgeon, K., Muthukumaran, G., Ding, D., Bajulaiye, A., Ferrari, V., & Libonati, J. R. (2015). Moderate-intensity treadmill exercise training decreases murine cardiomyocyte cross-sectional area. *Physiological Reports*, *3*(5), e12406. https://doi.org/10.14814/phy2.12406

Subedi, P., Schneider, M., Philipp, J., Azimzadeh, O., Metzger, F., Moertl, S., Atkinson, M. J., & Tapio, S. (2019). Comparison of methods to isolate proteins from extracellular vesicles for mass spectrometry-based proteomic analyses. *Analytical Biochemistry*, *584*, 113390. https://doi.org/10.1016/j.ab.2019.113390

Takaoka, M., & Miki, Y. (2018). BRCA1 gene: function and deficiency. *International Journal of Clinical Oncology*, *23*(1), 36–44. https://doi.org/10.1007/s10147-017-1182-2

Taki, H., Kashiwagi, A., Tanaka, Y., & Horiikc, K. (1996). Expression of intercellular adhesion molecules 1 (ICAM-1) via an osmotic effect in human umbilical vein endothelial cells exposed to high glucose medium. *Life Sciences*, *58*(20), 1713–1721. https://doi.org/10.1016/0024-3205(96)00151-8

Venkitaraman, A. R. (2019). How do mutations affecting the breast cancer genes BRCA1 and BRCA2 cause cancer susceptibility? *DNA Repair*, *81*, 102668. https://doi.org/10.1016/j.dnarep.2019.102668

Wallez, Y., & Huber, P. (2008). Endothelial adherens and tight junctions in vascular homeostasis, inflammation and angiogenesis. *Biochimica et Biophysica Acta (BBA) - Biomembranes*, *1778*(3), 794–809. https://doi.org/10.1016/j.bbamem.2007.09.003

Wang, L., Cheng, C. K., Yi, M., Lui, K. O., & Huang, Y. (2022). Targeting endothelial dysfunction and inflammation. *Journal of Molecular and Cellular Cardiology*, *168*, 58–67. https://doi.org/10.1016/j.yjmcc.2022.04.011

Wang, W., He, Q., Zhang, H., Zhuang, C., Wang, Q., Li, C., Sun, R., Fan, X., & Yu, J. (2021). A narrative review on the interaction between genes and the treatment of hypertension and breast cancer. *Annals of Translational Medicine*, *9*(10), 894–894. https://doi.org/10.21037/atm-21-2133

Wilkinson, E. L., Sidaway, J. E., & Cross, M. J. (2016). Cardiotoxic drugs Herceptin and doxorubicin inhibit cardiac microvascular endothelial cell barrier formation resulting in increased drug permeability. *Biology Open*, *5*(10), 1362–1370. https://doi.org/10.1242/bio.020362

Willis, M. S., Parry, T. L., Brown, D. I., Mota, R. I., Huang, W., Beak, J. Y., Sola, M., Zhou, C., Hicks, S. T., Caughey, M. C., D'Agostino, R. B., Jordan, J., Hundley, W. G., & Jensen, B. C. (2019). Doxorubicin Exposure Causes Subacute Cardiac Atrophy Dependent on the Striated Muscle–Specific Ubiquitin Ligase MuRF1. *Circulation: Heart Failure*, *12*(3). https://doi.org/10.1161/CIRCHEARTFAILURE.118.005234

Wolf, M. B., & Baynes, J. W. (2006). The anti-cancer drug, doxorubicin, causes oxidant stress-induced endothelial dysfunction. *Biochimica et Biophysica Acta (BBA) - General Subjects*, *1760*(2), 267–271. https://doi.org/10.1016/j.bbagen.2005.10.012

Woodcock, E. A., & Matkovich, S. J. (2005). Cardiomyocytes structure, function and associated pathologies. *The International Journal of Biochemistry & Cell Biology*, *37*(9), 1746–1751. https://doi.org/10.1016/j.biocel.2005.04.011

Yoshida, K., & Miki, Y. (2004). Role of BRCA1 and BRCA2 as regulators of DNA repair, transcription, and cell cycle in response to DNA damage. *Cancer Science*, *95*(11), 866–871. https://doi.org/10.1111/j.1349-7006.2004.tb02195.x

Yoshimura, M., Yasue, H., & Ogawa, H. (2001). Pathophysiological significance and clinical application of ANP and BNP in patients with heart failure. *Canadian Journal of Physiology and Pharmacology*, *79*(8), 730–735.

Zhang, L., Liu, L., & Li, X. (2020). MiR-526b-3p mediates doxorubicin-induced cardiotoxicity by targeting STAT3 to inactivate VEGFA. *Biomedicine & Pharmacotherapy*, *123*, 109751. https://doi.org/10.1016/j.biopha.2019.109751

Zhao, W., Wiese, C., Kwon, Y., Hromas, R., & Sung, P. (2019). The BRCA Tumor Suppressor Network in Chromosome Damage Repair by Homologous Recombination. *Annual Review of Biochemistry*, *88*(1), 221–245. https://doi.org/10.1146/annurev-biochem-013118-111058

Zheng, D., Liu, J., Piao, H., Zhu, Z., Wei, R., & Liu, K. (2022). ROS-triggered endothelial cell death mechanisms: Focus on pyroptosis, parthanatos, and ferroptosis. *Frontiers in Immunology*, *13*. https://doi.org/10.3389/fimmu.2022.1039241

Zhu, C., Hu, D. L., Liu, Y. Q., Zhang, Q. J., Chen, F. K., Kong, X. Q., Cao, K. J., Zhang, J. S., & Qian, L. M. (2011). Fabp3 Inhibits Proliferation and Promotes Apoptosis of Embryonic Myocardial Cells. *Cell Biochemistry and Biophysics*, *60*(3), 259–266. https://doi.org/10.1007/s12013-010-9148-2

Zhu, Y., Wu, J., Zhang, C., Sun, S., Zhang, J., Liu, W., Huang, J., & Zhang, Z. (2016). BRCA mutations and survival in breast cancer: an updated systematic review and meta-analysis. *Oncotarget*, *7*(43), 70113–70127. https://doi.org/10.18632/oncotarget.12158

Curriculum Vitae

Berk Umid Rasheed

Education

Bachelor of Science, Honors Specialization in Neuroscience Sept 2017 – April 2021
University of Western Ontario (UWO), London, ON

Master of Science, Anatomy and Cell Biology Sept 2021 – June 2023
University of Western Ontario (UWO), London, ON

Publications

- Microvessel stenosis, enlarged perivascular spaces and fibrinogen deposition are associated with ischemic periventricular white matter hyperintensities. A. Roseborough, **B. Rasheed**, Y. Jung, K. Nishimura, W. Pinsky, K. Langdon, R. Hammond, S. Pasternak, A. Khan, S. Whitehead. Published in Brain Pathology on August 13, 2021. DOI: 10.1111/bpa.13017.

- Transcriptomics of angiotensin II-induced long noncoding and coding RNAs in endothelial cells. Shuhan Bu, Hien C Nguyen, David C R Michels, **Berk Rasheed**, Sepideh Nikfarjam, Rohan Singh, Lynn Wang, Darshil A Patel, Shweta Singh, Mohammad Qadura, Krishna K Singh. Published in the Journal of Hypertension on July 1, 2022. DOI: 10.1097/HJH.0000000000003140

- Loss of fatty acid binding protein 3 ameliorates lipopolysaccharide-induced inflammation and endothelial dysfunction. Hien C Nguyen, Shuhan Bu, Sepideh Nikfarjam, **Berk Rasheed**, David C R Michels, Aman Singh, Shweta Singh, Caroline Marszal, John J McGuire, Qingping Feng, Jefferson C Frisbee, Mohammad Qadura, Krishna K Singh. Published in the Journal of Biological Chemistry on January 18, 2023. DOI: 10.1016/j.jbc.2023.102921

- Endothelial cell-specific loss of eNOS differentially affects endothelial function. Shuhan Bu, Hien Nguyen, David Michels, Sepideh Nikfarjam, **Berk Rasheed**, Sauraish Maheshkumar, Shweta Singh, Krishna Singh. Publisehd in PLoS One on September 23, 2022. DOI: 10.1371/journal.pone.0274487